ESCUELA SUPERIOR POLITÉCNICA DEL LITORAL

Facultad de Ingeniería Marítima, Ciencias Biológicas, Oceanográficas y Recursos Naturales

NUMERICAL HULL RESISTANCE CALCULATION OF A CATAMARAN USING OpenFOAM

GRADUATE PROJECT

In accordance with the requirements for the degree of

NAVAL ENGINEERING

BY

Diana Stephany Hurtado Bustos

Guayaquil – Ecuador

2016

ACKNOWLEDGEMENTS

My special appreciation to my mom, Piedad, my two older brothers, David y

Juan Carlos, for their entire support in every decision I made during my life

and career.

The people, that participated in my academic development, my teachers and

members of my collage. In especially to my advisor, Ruben Paredes.

And finally but not least important, my friends and everybody who

accompanied me during this time.

DEDICATION

I dedicate this project to my dad, Héctor, who has been my inspiration in life

and motivation during my career. To my nephews, Jesús Matías, Héctor,

Ariana y Juan David, by ask if I had finished my homework, because they

wanted to play with me.

DECLARATION

"I hereby declare that this thesis represents my own work which has been done after registration for the degree of Naval Architecture & Mechanical Engineer of Escuela Superior Politécnica del Litoral and all sources of knowledge used have been duly acknowledged. Escuela Superior del Litoral shall have the rights to preserve, use and disseminate this work in print or electronic format for academic or research purpose."

_____

Diana Stephany Hurtado Bustos

CERTIFIED BY

_____

Ph.D. Rubén Paredes

Thesis Supervisor

ABSTRACT

An accurate estimation of ship resistance is essential for the selection of the engines to achieve the required speed of navigation. In traditional ships, resistance is decomposed in frictional and wave components. In addition, for catamarans the interaction between its hulls has to be considered. In the present study, numerical resistance predictions using OpenFOAM were performed considering the Cormorant Evolution Catamaran, which provides travel services in the Galapagos Islands. These predictions were compared with experimental data published by Chávez and Lucín [1] and with systematic series [2].

Simulations were made at model scale of 2 [m] in two load conditions, considering demi and twin hull (S=0.56 [m]) configurations, following the experimental procedure done in [1]. A mesh convergence study was performed with 3 different meshes for V=1.05 [m/s] at Light Condition (T=0.086 [m]). The converged mesh, with 1 million of cells approximately, has the lower standard deviation and a 5% error when compared to its experimental value of 1.79 [N].

The errors between the experimental data and the numerical simulations for demi hull configuration were 43% and 36% for Light and Full conditions, respectively. Besides, for twin hull configuration the errors were around 14%

and 32% for Light and Full conditions, respectively. Finally, the numerical interference resistance of the catamaran was estimated and compared with Yokoo and Tasaki method [3], experimental data [1] and Maxsurf simulations showing a similar behavior.

LIST OF CONTENTS

LIST OF FIGURES

LIST OF TABLES

NOMENCLATURE

B	Beam [m]
B_{cat}	Catamaran beam [m]
B_{WL}	Beam at water line [m]
C_B	Block coefficient
CFD	Computational Fluid Dynamics
C_M	Middle section coefficient
C_{PL}	Prismatic coefficient
CT	Total resistance coefficient
D	Depth [m]
DTC	Duisburg Test Case
Fn	Froude number
I_{xx}	Inertia [kg.m^2]
k	Turbulent kinetic energy [m^2/s^2]
L	Length [m]
L_{pp}	Length between perpendiculars [m]
L_{WL}	Length at water line [m]
M	Mass [kg]
P	Pressure [k/m.s^2]
RANS	Reynolds Average Navier Stoke
Re	Reynolds number
R_T	Total resistance [N]
s	length between hulls [m]
S_W	wet surface [m^2]
t	time [s]
T_M	Draft [m]
U	Fluid velocity [m/s]
v	Velocity [m/s]
V	Volume [m^3]
VoF	Volume of Fluid
y+	Y Plus
z	Sinkage [m]
λ	Scale factor
Δ	Displacement [ton]
ρ	Density [kg/m^3]
μ	Viscosity m^2/s]
ω	Dissipation ratio [1/s]

INTRODUCTION

In Ecuador, Catamarans are the most popular ship design used for tourism, especially in Galapagos Islands. This is mainly because of its improved transversal stability, a better passenger and crew comfort, and the reduced draft that minimize ship resistance and its environmental impact when compared to mono-hulls ships.

In general, ship resistance estimation is a complex task. It can be decomposed in frictional and residual components. Besides, there is an additional component for the catamaran, such as the interference between the demi-hulls. There are three different methods to predict ship resistance. The first one is the empirical method [4]. This is the simplest and fastest technique, but it works only at the earliest design stage with a lack of precision and some restrictions concerning to the type of ship or principal dimensions of it. The following alternative is model testing; this is more reliable and accurate than the empirical method. However, it can be expensive in terms of production of several scale models, the amount time by each test, and the requirement of Froude and Reynolds numbers similarity between models and real ship. In the last years, numerical simulations using Computational Fluid Dynamics (CFD) have become a third alternative used in the industry. However, it cannot be used as a black box because it can

produce spurious results if not set correctly. It is required to perform a verification and validation procedure, usually using experimental data.

GENERAL OBJECTIVE

Calculate the total resistance of the Cormorant Evolution Catamaran sailing in deep water using an open-source code, know as: OpenFOAM (CFD).

SPECIFIC OBJECTIVES

- Understand the basic principles of CFD method used to calculate the ship resistance.
- Define the minimum mesh density required using a Demi Hull and applying symmetry or Two Hulls to achieve an acceptable accuracy.
- Perform numerical calculation of total resistance and its interference component of Catamaran "Cormorant Evolution" for Froude number between 0.24 and 0.34.

METHODOLOGY

In this work, numerical simulations were performed to predict total resistance of a catamaran and results were validated using experimental data obtained by Chávez and Lucín [1]. This document contains 3 chapters. The first chapter describes the Catamaran characteristics, and the experiments done in the Lake of ESPOL. In chapter 2, numerical method is described, including the steps required in the simulations. The DTC benchmark hull geometry is used to understand the simulation procedure. Next, in chapter 3, the results of the Catamaran are presented and compared with available resistance experimental data.

BENEFITS OF CFD ANALYSIS

In the past, the design of new ships relied on existing ships. This means that ship designers learned about the problems and its possible solutions from previous experiences. However, this process is slow and expensive. One alternative to develop a new ship design is to run experimental test to optimize its geometry before the construction. Nevertheless, a modern and cheaper alternative is the use of computational tools. The CFD solution is a numerical method to solve the nonlinear differential equations governing the fluid flow.

Computational Fluid Dynamics (CFD) techniques are used to analyze fluid flow related problems in different industries. For example: aerospace, automotive, marine, medical. Some advantages of this method are:

i.   Time and cost reduction of new designs.

ii. Reduction of the number of design variants in a matrix.

iii. Analyze different problems whose experiments are difficult and/or dangerous.

iv. Relative easy to optimize designs.

However, users need some knowledge on the underlying physics and training to identify the limitations of the numerical tool. This is because if the CFD analysis is not setup correctly, it can produce spurious results.

Due to all this benefits, this method has become popular on engineering designs. There are several companies that have developed computational packages that implements general CFD methods, and others that only focus on specific fluid problems. Next, there is a list of some software typically use for CFD simulations:

ANSYS-CFX	http://www.ansys.com	Commercial
FLUENT	http://www.fluent.com	Commercial
STAR-CD	http://www.cd-adapco.com	Commercial
FEMLAB	http://www.comsol.com	Commercial
FEATFLOW	http://www.featflow.com	Open source
OpenFOAM	http://www.openfoam.com	Open source

In this thesis, OpenFOAM is used to predict the catamaran resistance. OpenFOAM is a free, open source CFD software developed primarily by OpenCFD Ltd since 2004, distributed by OpenCFD Ltd and the OpenFOAM Foundation [5]. It was chosen because of its ability of customization, there is online training and support and it is an open source code.

CHAPTER 1

EXPERIMENTAL CATAMARAN DATA

In this chapter, the catamaran characteristics and experimental data are described. The latter will be used for validation of numerical results.

1.1 RESISTANCE ESTIMATION

The resistance of a ship at a given speed is the force required to tow the ship at that speed in calm water, assuming no interference from the towing ship [4]. The ship must perform the minimum shaft horsepower to cruise at required velocity. The total ship resistance is made up of several components. This can be divided in frictional and residual resistance. Frictional resistance is produced due the motion of the hull through a viscous fluid. Residual resistance is produced due pressures around the hull for waves and the type of fluid, as shown in Figure 1.

Figure 1: Decomposing resistance into components
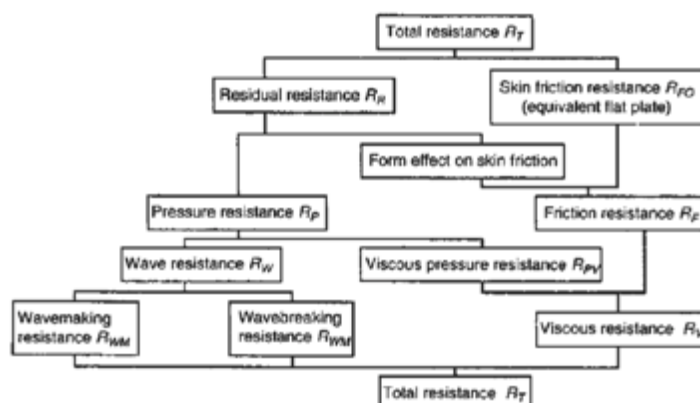
Source: Bertram V. [6]

1.2 CATAMARAN MAIN CHARACTERISTICS

Catamarans are ships with two parallel hulls of equal size, joined by a frame or superstructure. The division of the water plane area offers a good stability quality [4]. See Figure 2.

Figure 2: Catamaran Cormorant Evolution

Source: Cormorant Cruise [7]

The "Cormorant Evolution" Catamaran was built in Ecuador in 2011 by "Astilleros y Marina BOTTO CIA. LTDA", and operates through "Cormorant Cruise" in Galapagos Islands [7]. It's a 32.5 [m] length fiberglass touristic vessel; with a "V" middle section, a bulbous bow, separation of 9.11[m] between the centerlines of hulls and a design velocity of 5.14 meters per second (10 knots).

Later, a model of 2 [m] length was build using Cormorant Evolution hull-shape, to measure experimental resistance in the lake of "Escuela Superior Politécnica del Litoral" (ESPOL) [1]. The scale factor was of λ=16.25. The experiment velocity range of the model was considerate from 1.05 to 1.45 meter per second. Table 1 shows the main characteristics of the catamaran at two load conditions.

Table 1: Main Characteristics of Prototype and Model.

	LIGHT LOAD		FULL LOAD	
	Catamaran	**Model**	**Catamaran**	**Model**
L [m]	32.50	2.00	32.50	2.00
L_{wl} [m]	30.21	1.87	30.42	1.89
B_{cat} [m]	12.20	0.751	12.20	0.751
B [m]	3.09	0.19	3.09	0.19
s [m]	9.11	0.561	9.11	0.561
D [m]	3.52	0.22	3.52	0.22
T [m]	1.40	0.086	1.66	0.103
Δ [ton]	58.52	0.018	78.74	0.024
V [m³]	57.09	0.018	76.84	0.023
S_w [m²]	115.39	0.51	131.99	0.56
LCB [m]	-1.229	-0.04	0.815	-0.04
v [kn]	10.00	2.48	10.00	2.48
F_n	0.298	0.298	0.296	0.296
C_b	0.567	0.567	0.604	0.604
C_m	0.739	0.739	0.756	0.756
C_{pl}	0.767	0.767	0.798	0.798

Source: Chávez and Lucín [1]

1.2 EXPERIMENTAL SHIP RESISTANCE DATA

The hulls of the model were built on fiberglass and joined it with an aluminum and wood structure. The model was towed from a boat in the lake of ESPOL and the resistance force (drag) was recorded. The test was performed considering two load conditions at different speeds. In Chávez and Lucín work [1], an aluminum boat was used to tug the model. The tug arm length is 3.20 [m], the model length is 2 [m], the power of the outboard engine 6 [HP] and the dimensions of the boat are: length L=4.3 [m] and beam B=1.6 [m]. Figure 3 show the distribution of equipment's to experimental tests.

Figure 3: Experimental test equipment's distribution
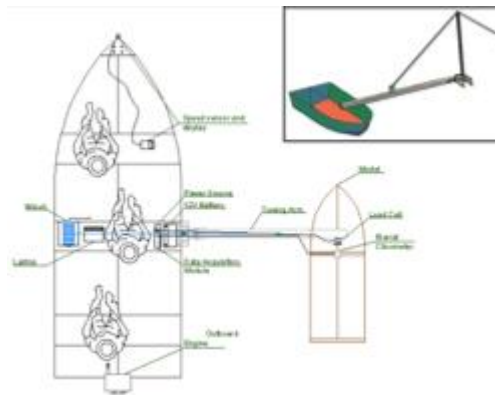
Source: Benítes D. [18]

Figure 4 and Table 2 describes the equipment used on the experimental test:

Figure 4: Experimental test equipment
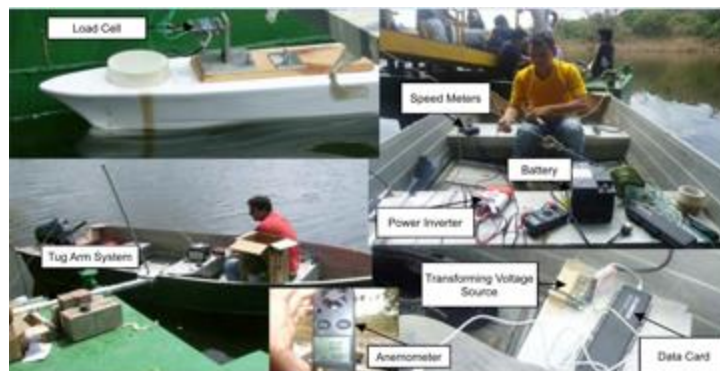
Source: Chávez and Lucín [1]

Table 2: Experimental Test Equipment

EQUIPMENT	CHARACTERISTICS
Battery	MOTOREX, 12 [V], 700 [A]
Power Inverter	BLACK & DECKER, Model PI500BB
Transforming voltage source	COSEL CO. LTD. Model K15A-12
Data card	OMEGA, Model OMB-DAQ-3000
Load cell	AMCELLS, Model STL S-Type 50 [lb]
Speed meters	SWOFFER INSTRUMENTS INC. Model 2100-STDX 2100-LX
Anemometer	INTELL INSTRUMENTS PLUS. Model AR816A

Source: Chávez and Lucín [1]

In the experiments, a single hull (demi-hull) was used first and then both hulls were considered with three separations: reduce 50.5 [cm], original 56.1 [cm] and increased 61.7 [cm].

1.2.1 Experimental Test

The procedure followed in the experimental tests was:

i. Record the initial value of the Load Cell when the model is not moving forward and set it as the cero point.

ii. Accelerate the outboard of the boat until the speed is stabilized.

iii. Record the forces for 60 seconds with a rate of 120 [Hz].

iv. At the same time window, record the wind velocities with the anemometer and the wake with a sternpost speed meter.

v. Repeat the process for different velocities and load conditions.

Figure 5 shows one of the experimental tests done at ESPOL Lake.

Figure 5: Experimental twin hull test at ESPOL lake in Full Load Condition

Source: Chávez and Lucín [1]

1.2.2 Demi Hull Resistance Test Results

The following tables show the average experimental results and its standard

deviation obtained for a demi and twin hull at two load conditions.

Table 3: Experimental Results of a Demi-Hull Light Condition

v [m/s]	Wind Vel. [m/s]	Avg. Force [mV]	Force [kg]	% Sta. Dev.
0.00	0.10	4.64	0.000	13.4
1.05	0.95	4.93	0.183	12.6
1.14	1.34	-	0.399	-
1.20	1.20	5.18	0.367	12.7
1.30	1.40	-	0.537	-
1.45	1.55	5.71	0.715	9.6

Source: Chávez and Lucín [1]

Table 4: Experimental Results of a Demi-Hull Full Load

v [m/s]	Wind Vel. [m/s]	Avg. Force [mV]	Force [kg]	% Sta. Dev.
0.00	0.00	6.48	0.000	9.88
1.03	1.13	6.93	0.315	9.23
1.10	1.20	-	0.421	-
1.23	1.28	7.16	0.467	9.08
1.35	1.45	-	0.570	-
1.45	1.35	5.52	0.715	8.64

Source: Chávez and Lucín [1]

1.2.3 Two Hull Resistance Test Results

Although three hulls separations were considered in the experimental work.

Only results of the original separation are reported here, because it has the

lowest resistance interference. For the model, the separation was of 0.561

[m]. The experiment follow the same steps describe in Section 1.2.1. The experimental results of two hulls for two load conditions are:

Table 5: Experimental Results of Two joined Hulls Light Condition

v [m/s]	Wind Vel. [m/s]	Avg. Force [mV]	Force [kg]	% Sta. Dev.
0.00	0.00	3.01	0.000	25.9
1.05	0.95	3.77	0.521	15.9
1.14	1.04	-	0.490	-
1.26	1.16	3.92	0.627	20.2
1.32	1.32	-	0.792	-
1.47	1.37	4.21	0.826	18.1
1.53	1.73	-	1.053	-
1.76	1.46	-	1.232	-
1.94	1.84	-	1.356	-

Source: Chávez and Lucín [1]

Table 6: Experimental Results of Two joined Hulls Full Condition

v [m/s]	Wind Vel. [m/s]	Avg. Force [mV]	Force [kg]	% Sta. Dev.
0.00	0.00	2.69	0.000	26.77
1.05	0.95	3.87	0.807	18.09
1.12	1.12	-	0.702	-
1.25	1.55	4.19	1.027	15.75
1.33	1.53	-	1.075	-
1.46	1.36	4.49	1.239	15.14
1.55	1.55	-	1.484	-
1.75	1.55	-	2.104	-

Source: Chávez and Lucín [1]

1.2.4 Experimental test results

Figure 6 shows experimental resistance data as a function of speed and its corresponding trend line using a second order polynomial for the demi hull in

both load conditions. The correlation factor of data goes from 0.9424 to 0.9968; this means that the data are reliable.

Figure 6: Resistance of a Demi-Hull in Light and Full Condition
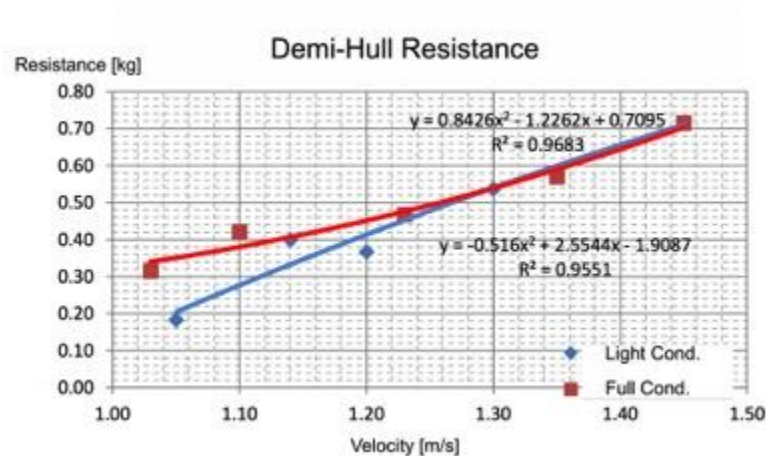
Source: Chávez and Lucín [1]

Both conditions are very closed after 1.3 [m/s], because the bulbous increase the resistance due it is not completely submerged at light condition. Figure 7 shows the resistance for the whole catamaran considering two hulls in both load conditions.

Figure 7: Resistance of Two Hull in Light and Full Condition
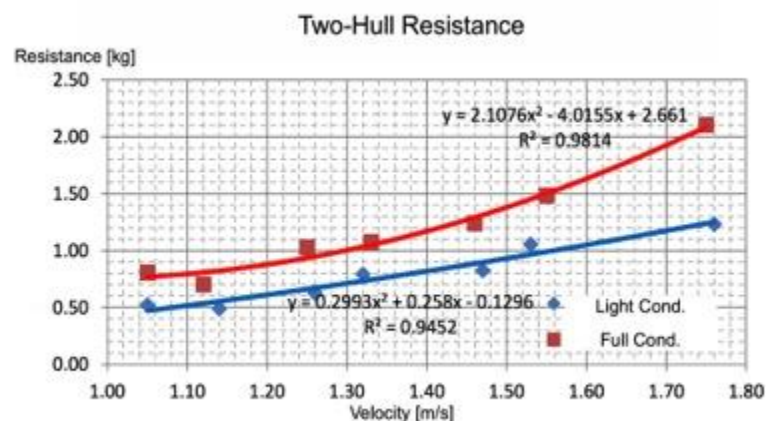
Source: Chávez and Lucín [1]

From Figure 7, the resistance in full load condition is greater than light load condition. This is expected because of its increase wetted area surface.

CHAPTER 2

NUMERICAL METHOD – CFD

In this chapter, a general overview of OpenFOAM is described, including how it works, the meshing procedure for the model and computational domain. Also, the DTC hull tutorial is explained as a first exercise to understand the use of this numerical tool applied to ship resistance calculations. Figure 8 shows the workflow of OpenFOAM.

2.1 OPENFOAM SOFTWARE DESCRIPTION

2.1.1 General Aspects

Open Source Field Operation and Manipulation (OpenFOAM) is a free source code with C++ programing language. This code creates executable scripts, called *applications* which are divided in two categories: *solvers* developed for specific problems in continuum mechanics, and *utilities* developed to manipulate data. The software can be downloaded from www.openfoam.com. It has several solvers and utilities developed and tested by OpenCFD Ltd. and ESI-OpenCFD's Application Specialists, which covers a wide range of problems [5]. Also, it is possible to develop new solvers and utilities of OpenFOAM. The work sequence of OpenFOAM can be classified in three fundamental steps, described in Figure 9.

Figure 8: OpenFOAM workflow
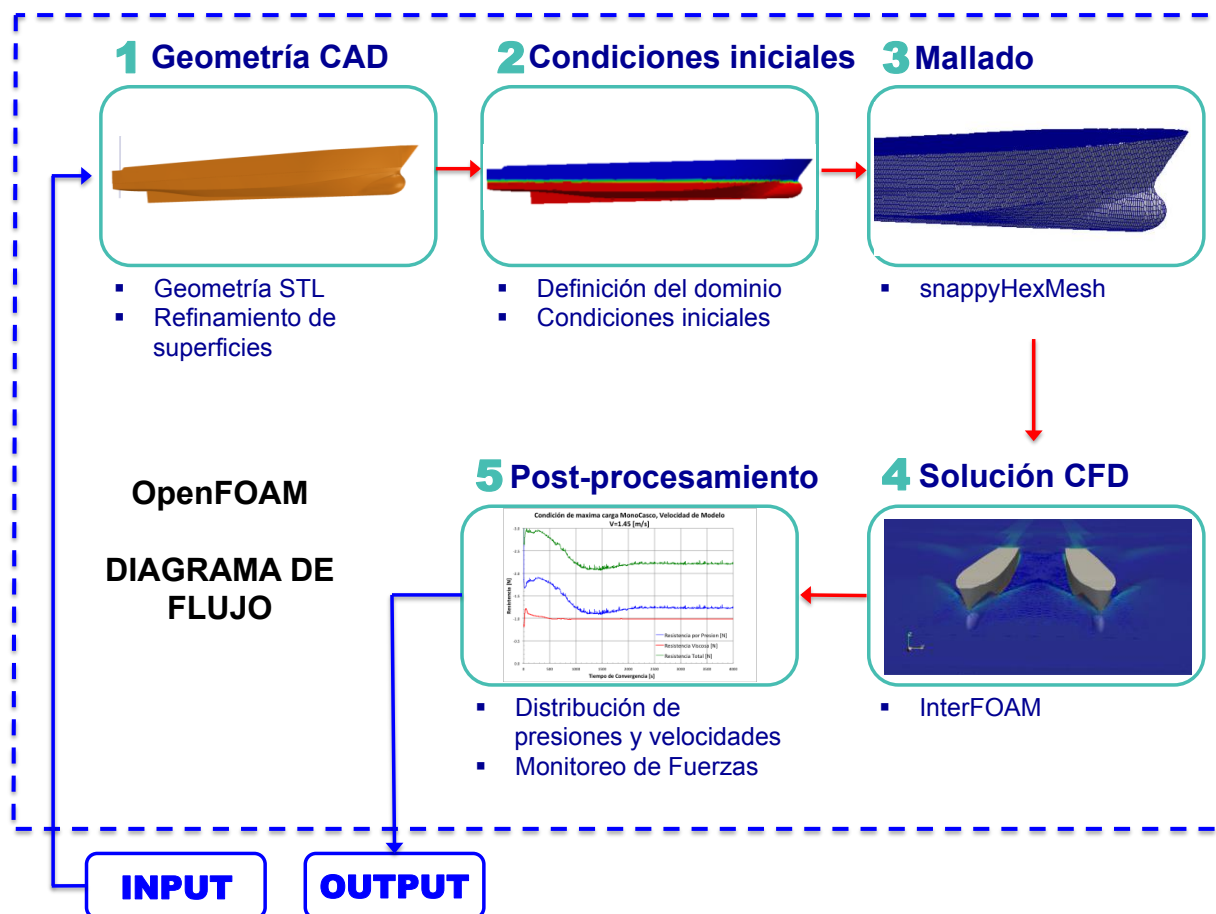
Figure 9: Overview of OpenFOAM structure
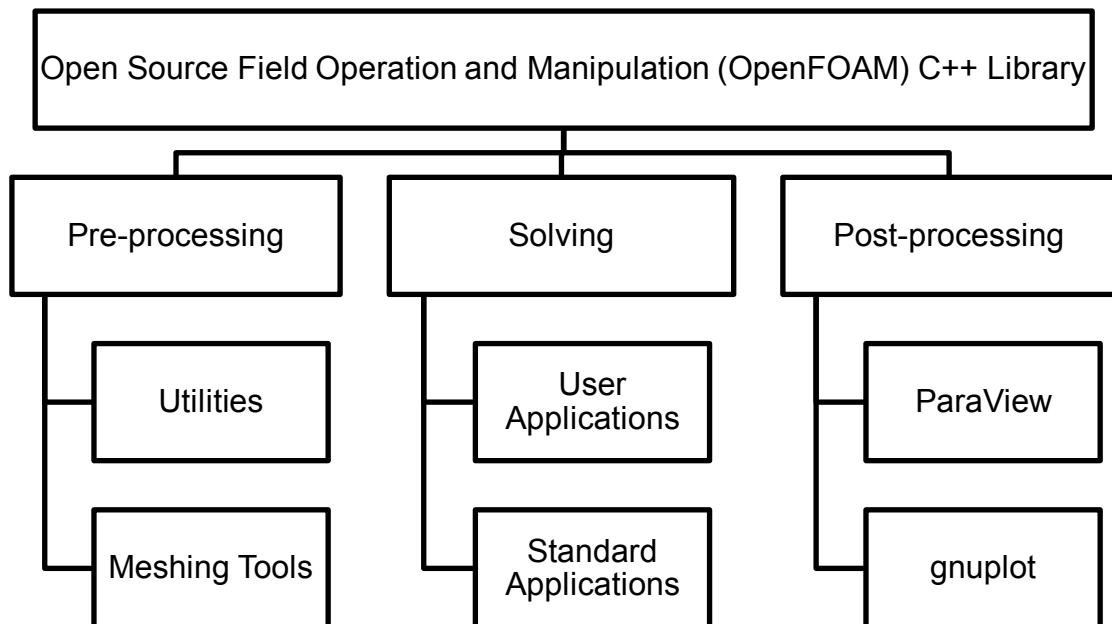
These three fundamental steps are Pre-processing, Solving and Post-processing that explained in the Section 2.1.2. OpenFOAM basic directory structure is shown in Figure 10 and it contains a set of file distributed in three directories: 0.org, system and constant. The *constant* directory has a full description of the case geometry and physical properties of fluids. The *system* directory has files of the solution procedure, basics files are: *controlDict, fvSchemes and fvSolution*. The 0.org directory has the constants, as: velocity, kinematic turbulence viscosity, pressure and turbulent kinetic energy.

Figure 10: Case directory structure
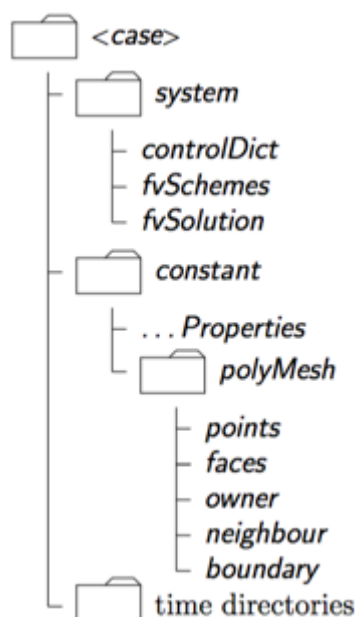
Figure 11 contains the standard set of keyboard entries of all data file of OpenFOAM. This entry provides a brief description of the each file, as: the format version, the data formant (ascii or binary), the class of data file (typically *dictionary*) and the object or file name.

Figure 11: Header data file by OpenFOAM

```
/*--------------------------------*- C++ -*----------------------------------*\
| =========                 |                                                 |
| \\      /  F ield         | OpenFOAM: The Open Source CFD Toolbox           |
|  \\    /   O peration     | Version:  3.0.x                                 |
|   \\  /    A nd           | Web:      www.OpenFOAM.org                      |
|    \\/     M anipulation  |                                                 |
\*---------------------------------------------------------------------------*/
FoamFile
{
    version     2.0;
    format      ascii;
    class       dictionary;
    object      blockMeshDict;
}
// * * * * * * * * * * * * * * * * * * * * * * * * * * * * * * * * * * * * * //
```

2.1.2 Simulation Procedure

There are three main steps to perform a simulation. First, Geometry, Boundary and Initial conditions of the problem are defined in the Pre-processing. Later, standard solvers solve the governing equations according to the flow problem. Finally, results are reviewed in the Post-processing.

Pre-Processing

The pre-processor provides all the required data to define a flow problem in OpenFOAM. The input data is specified in text files and includes:

i. Mesh generation that discretizes the domain into smaller elements, called cells.

ii. Fluid properties.

iii. Physical models to the simulation: Laminar or turbulent flow.

iv. Define boundary conditions.

v. Geometry definition of the problem, computational domain.

OpenFOAM support STereoLithography files (STL) to describe surface geometry in 3D. The mesh quality of the geometry is an important part of the numerical solution. The higher the mesh quality, the better the results accuracy. But, this also demands more the computational resources and CPU time to solve them.

<u>Solving</u>

OpenFOAM developed the following standard solvers depending on the flow characteristics:

i. 'Basic' CFD codes

ii. Incompressible flow

iii. Compressible flow

iv. Multiphase flow

v. Direct numerical simulation (DNS)

vi. Combustion

vii. Heat transfer and buoyancy-driven flows

viii. Particle-tracking flows

ix. Molecular dynamics methods

x. Direct simulation Monte Carlo methods

xi. Electromagnetics

xii. Stress analysis of solids

For marine applications, two solvers can be used for multiphase flows, interFoam and interDyFoam. In this thesis, the InterFoam solver is applied because only ship resistances are measured in experiments. InterFoam is a solver for two incompressible, isothermal immiscible fluids using a volume of fluid phase-fraction based interface capturing approach [8]. The computational domain includes fresh water and atmosphere.

Post-Processing

Results are visualized using ParaView is an open source tool. ParaView operate a tree-based structure in which data can be filtered from the top-level case module to create sets of sub-modules [8]. Figure 12 is the user interphase of ParaView, where are four default layouts: upper toolbar, layout, pipeline browser and properties.

Figure 12: ParaView User Interphase
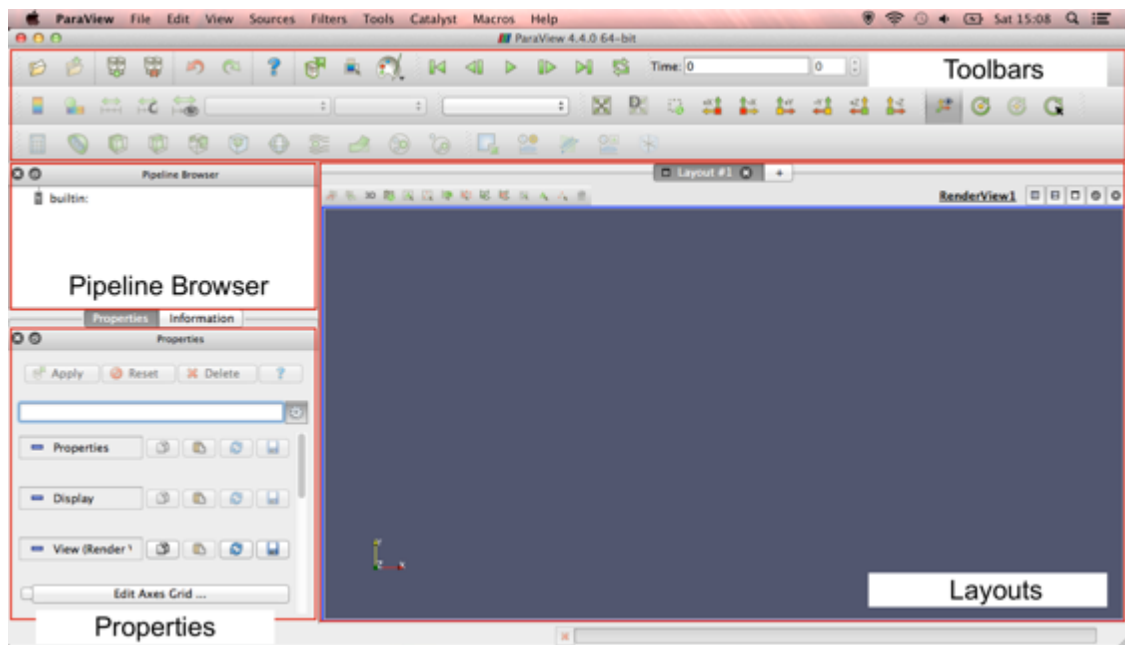
Menu Bar:	Allows the access to all the features.
Toolbars:	Quick access to the features.
Pipeline Browser:	Management and filter of data, shows the pipeline structure.

Panel Properties: Viewer and ability to changes parameters of the current pipeline object. The properties are by default match with an INFORMATION tab.

Layout: 3D geometry viewer.

Figure 13 is the quick access toolbar, which provide user the capacity of add and edit data parameters.

Figure 13: ParaFOAM toolbar
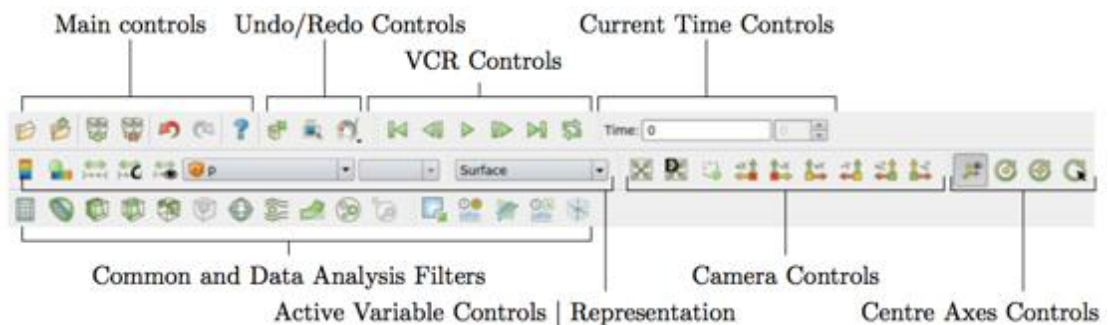
2.2 DESCRIPTION OF DTC HULL TUTORIAL

In general, numerical simulations are validated using benchmark cases. In the naval field there are 4 geometries that are typically used. Namely, Duisburg Test Case (DTC), Wigley, JAPAN Bulk Carrier (JBC), and Surface Combatant DTMB Model 5415. OpenFOAM 3.0x version offers a tutorial with the DTC geometry. DTC is a 14,000 TEUs post-panamax container carrier developed by the Institute of Ship Technology, Ocean Engineering and Transport System (ISMT) from Duisburg-Essen University, Germany [9]. Figure 14 shows the tree directory of DTC Hull case, which contains three folders,

where each one contains text files and folders with different parameters used to setup the case.

Figure 14: DTC tree directory case
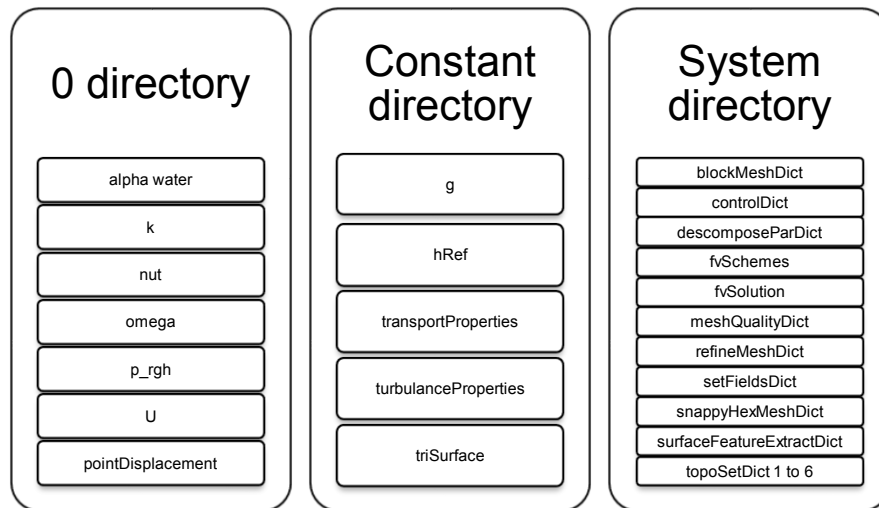
2.2.1 Hull Geometry

DTC is a single screw vessel, with bow bulbous, large bow flare, large stern overhang and transom. The main dimensions and load condition are described in Table 7:

Table 7: DTC Dimensions

	Model	**Full Scale**
L_{pp} **[m]**	5.976	355.0
B_{wl} **[m]**	0.859	51.0
D [m]	0.575	34.16
T_m **[m]**	0.244	14.5
V [m³]	0.827	173467.0
C_b	0.661	0.661
S_w **[m²]**	6.243	22032.0
v [m/s]	1.66	12.86
Fn	0.218	

Source: Moctar, Shigunov & Zorn [9]

Figure 15 show the 3D model used in OpenFOAM Tutorial that corresponds to model size scale at about 1:60. The model is generated on CAD software, Rhinoceros.

Figure 15: Perspective view of DTC Hull

2.2.2 Domain Geometry

The physical domain surrounding the vessel is modeled in the computational fluid domain and it is composed by air and water. Also, considering that the ship moves in a straight line, only half of the domain of *y* plane, fluid and hull, is modeled to save computational time. Figure 16 shows the principal dimensions of the domain, including the ship geometry and two fluids. The dimensions are expressed as a length between perpendiculars (L_{pp}) ratio.

2.2.3 Mesh Generation

Mesh is generated in two steps to divide the computational domain in small pieces, named cells, using two files: *blockMeshDict* and *snappyHexMeshDict*.

Figure 16: Domain size
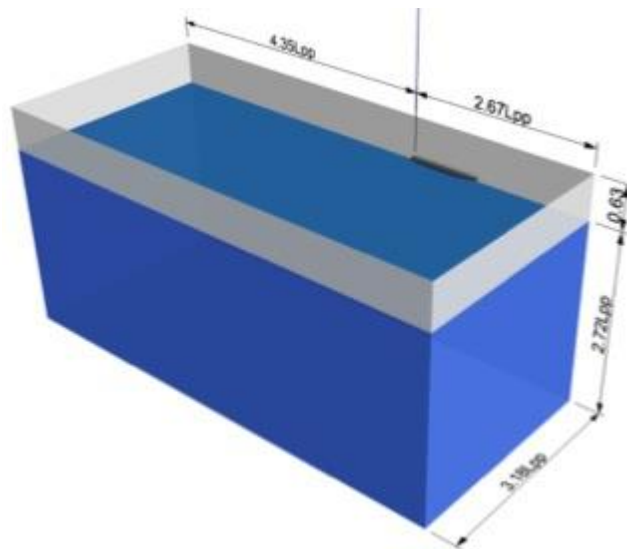
In the first step, BlockMeshDict file creates a background mesh with blocks using vertices (points). For example, the following block is defined as hexagonal with 42, 19 and 50 cells in the x, y, and z direction respectively. Finally a simpleGrading expansion type and its ratio are reviewded.

Hex (0 1 2 3 4 5 6 7) (42 19 50) simpleGrading (1 1 0.05)

In this work, the fluid domain is decomposed in 6 blocks with different cells density to improve results accuracy, see Figure 17.

In the second step, SnappyHexMesh inserts the DTC hull geometry (STL format) into the mesh background. Figure 18 shows a slide of the mesh around bolbuos and the stern of DTC Hull case.

Figure 17: Mesh distribution for DTC Hull
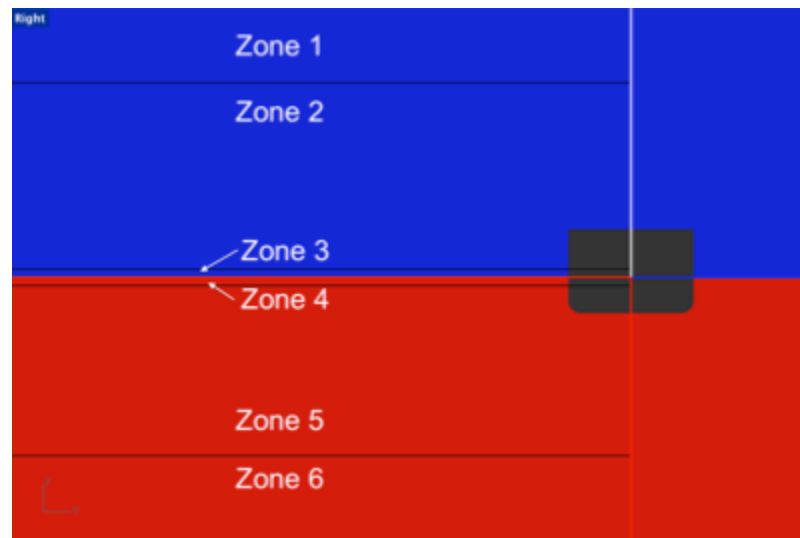
Figure 18: Mesh generate in DTC Hull
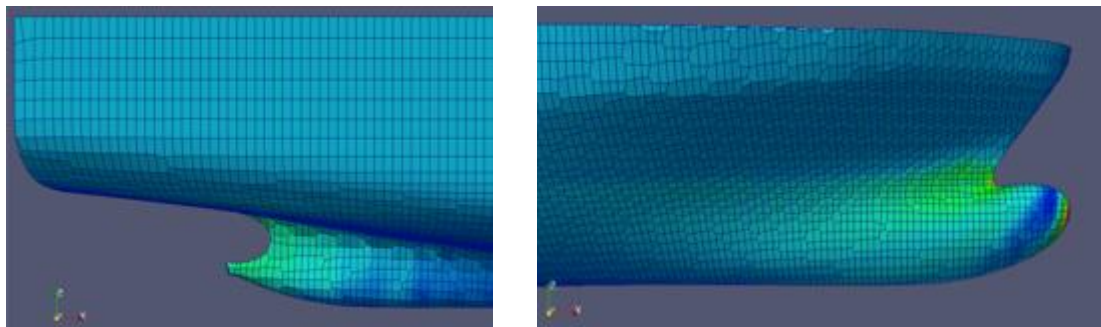
To capture the free surface interface, air and water, the volume of fluid (VoF) algorithm is used. This requires additional refinement on 3 and 4 zones. Toposet files create boxes around the hull and generate other zones of refinement. Figures 19 and 20 shows six boxes created by Toposet files.

2.2.4 Governing Equations

There are three physical laws that govern a fluid flow: Conservation of Mass, Conservation of momentum, and Newton's Second Law. However, these equations cannot be solved analytically for all kind of problems.

Figure 19: Topo Sets of Longitudinal slide
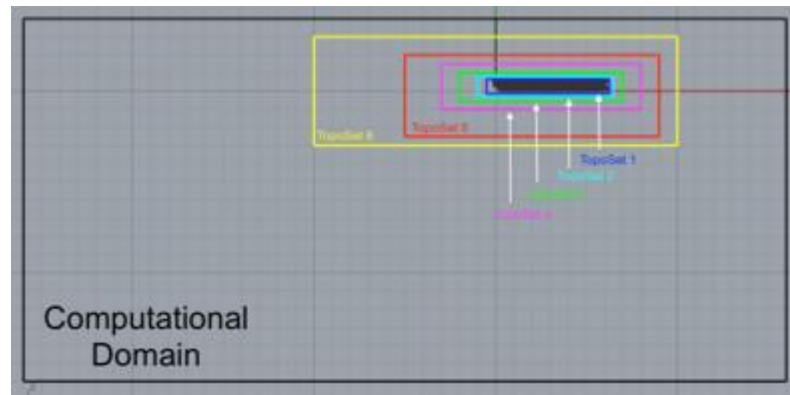
Figure 20: Perspective view of Topo Set
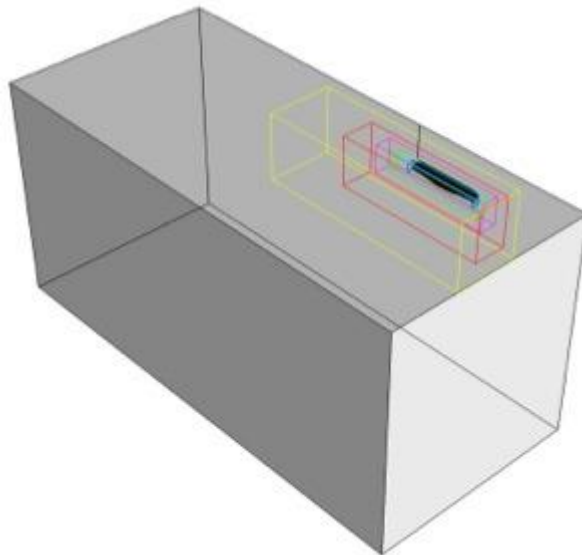
One alternative is to solve them numerically using Computational Fluid Dynamics (CFD). There are different methods to compute a turbulent flow depending the process of modeling: Direct Numerical Simulation (DNS), Large Eddy Simulation (LES) and Reynolds Average Navier-Stokes (RANS). Figure 21 shows a comparison between these methods.

Figure 21: Multi-scale and Multi-resolution approaches for turbulence
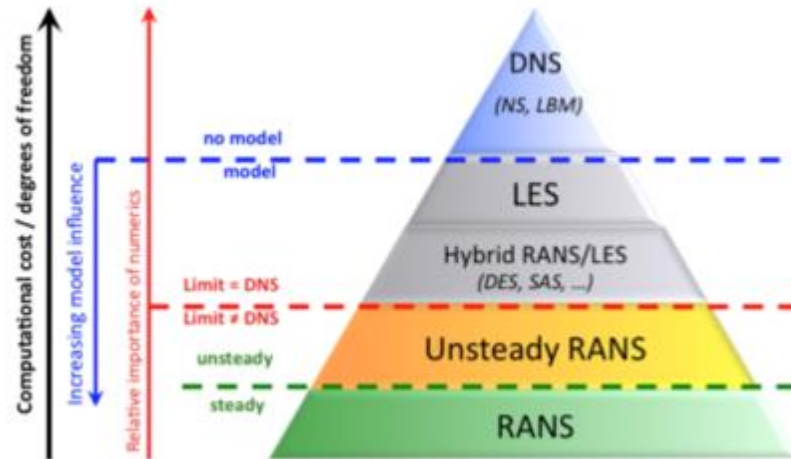
Source: Laval [9]

In real applications, fluids flow is turbulent and it can be modeled by RANS technique.

The equations for conservation of mass and momentum are:

$$\frac{\partial u_i}{\partial x_i} = 0 \tag{1}$$

$$\rho \frac{\partial u_i}{\partial t} + \rho u_j \frac{\partial u_i}{\partial x_i} = -\frac{\partial p}{\partial x_i} + \frac{\partial t_{ji}}{\partial x_j} \tag{2}$$

The vector u_j and x_i are velocity and position, *t* is time, *p* is pressure, *ρ* is the density and t_{ji} is the viscous stress tensor defined by:

$$t_{ji} = 2\mu s_{ij} \tag{3}$$

Where μ is molecular viscosity and s_{ij} is the strain-rate tensor,

$$s_{ij} = \frac{1}{2}\left(\frac{\partial u_i}{\partial x_j} + \frac{\partial u_j}{\partial x_i}\right) \tag{4}$$

Rewriting the equation in a conservative form:

$$u_j \frac{\partial u_i}{\partial x_j} = \frac{\partial}{\partial x_j}(u_j u_i) - u_i \frac{\partial u_j}{\partial x_j} = \frac{\partial}{\partial x_j}(u_j u_i) - u_i \tag{5}$$

Combining equations (2) through (5) generate the Navier-Stokes equations in conservative form:

$$\rho \frac{\partial u_i}{\partial t} + \rho \frac{\partial}{\partial x_j}(u_j u_i) = -\frac{\partial p}{\partial x_i} + \frac{\partial}{\partial x_j}(2\mu s_{ji}) \tag{6}$$

2.2.5 Turbulence modeling

The Reynolds averaging process represents the three velocity components as a slowly varying mean velocity with a rapidly fluctuating turbulent velocity around it. It also introduces six new terms, known as Reynolds stresses. Equation (6) can be rewritten to become the Reynolds averaged equations of motion in conservative form. Equation (7) is usually referred as the Reynolds-average Navier-Stokes equation (RANS) [11].

$$\rho \frac{\partial U_i}{\partial t} + \rho U_i \frac{\partial U_i}{\partial x_j} = -\frac{\partial P}{\partial x_i} + \frac{\partial}{\partial x_j}\left(2\mu s_{ji} - \rho \overline{u_j' u_i'}\right) \tag{7}$$

The quantity $-\rho \overline{u_j' u_i'}$ is known as the Reynolds-stress tensor.

These new terms represents the increase in effective fluids velocity due to the existence of turbulent eddies in the flow. The introduction of turbulence models helps to represent the interaction between the Reynolds stresses and the underlying mean flow, and to close the system of RANS equations [12].

For linear eddy viscosity models, RANS need some extra terms (transport properties) to represents the turbulence properties of the flows. These extra terms are listed in Table 8 for linear eddy viscosity models:

Table 8: RANS based turbulence for linear Eddy viscosity models

Nº of Extra Transport Equations	Name
Algebraic models	Cebeci-Smith model Baldwin-Lomax model Johnson-King model A roughness-dependent model
One equation models	Prandtl's one-equation model Baldwin-Barth model Spalart-Allmaras model
Two equation models	k-epsilon models k-omega models Realisability issues

In this work turbulence is modeled using the k-Omega SST method, which is a two-equation linear eddy-viscosity model. This turbulence model is more accurate and reliable for cases where exits adverse pressure gradient flows [12]. The first transport variable is turbulent kinetic energy, k, the second transport variable is the specific dissipation SST is the Shear Stress Transport, which differs from the k-Omega standard model by:

i. Graduals change from the standard k-Omega model in the inner region of the boundary layer to the k-epsilon model in the outer part of the boundary layer.

ii. Includes a modified turbulence viscosity equation for the transport effects of the turbulence shear stress.

The Governing equations for k-omega SST model are:

Turbulence kinetic energy $\frac{\partial k}{\partial t} + U_j \frac{\partial k}{\partial x_j} = P_k - \beta^* k \omega + \frac{\partial}{\partial x_j}\left[(\nu + \sigma_k \nu_T)\frac{\partial k}{\partial x_j}\right]$ (8)

Specific dissipation rate

$$\frac{\partial \omega}{\partial t} + U_j \frac{\partial \omega}{\partial x_j} = \alpha S^2 - \beta \omega^2 + \frac{\partial}{\partial x_j}\left[(v + \sigma_\omega v_T)\frac{\partial \omega}{\partial x_j}\right] + 2(1 - F_1)\sigma_{\omega 2}\frac{1}{\omega}\frac{\partial k}{\partial x_i}\frac{\partial \omega}{\partial x_i} \quad (9)$$

F1 (Blending Function) $F_1 = tanh\left\{\left\{min\left[max\left(\frac{\sqrt{k}}{\beta^*\omega y},\frac{500v}{y^2\omega}\right),\frac{4\sigma_{\omega 2}k}{CD_{k\omega}y^2}\right]\right\}^4\right\}$ \quad (10)

Note: F1= 1 inside the boundary layer and 0 in the free stream.

$$CD_{k\omega} = max\left(2\rho\sigma_{\omega 2}\frac{1}{\omega}\frac{\partial k}{\partial x_i}\frac{\partial \omega}{\partial x_i}, 10^{-10}\right) \quad (11)$$

Kinematic eddy viscosity $v_T = \frac{a_1 k}{max(a_1\omega, SF_2)}$ \quad (12)

F2 (Second Blending Function) $F_2 = tanh\left[\left[max\left(\frac{2\sqrt{k}}{\beta^*\omega y},\frac{500v}{y^2\omega}\right)\right]^2\right]$ \quad (13)

2.2.5 Boundary and Initial Conditions

The following assumptions about the numerical model to implement, are considered:

   i.   Steady, turbulent and three-dimensional flow.

   ii.   Single-phase flow.

   iii. Uniform velocity.

   iv.   Constant air and water properties

Boundary conditions are defined into blockMeshDict. These boundaries include atmosphere, inlet, outlet, bottom, side, and midPlane. The initials conditions are described in *0* and *constant* folders. The 0 directory includes velocity (U) and pressure (p) files. The constant directory includes transport and turbulence properties. For the transport properties the values for viscosity (*nu*) and density (*rho*) are shown in Table 9:

Table 9: Transport properties

Air	Nu	1.48 * 10⁻⁵	m²/s
	Rho	1.000	Kg/m³
Water	Nu	1.09 * 10⁻⁶	m²/s
	Rho	0.988	Kg/m³

Turbulence is modeled as a Reynolds-Averaged Simulation with kOmegaSST model; these turbulences parameters have values according to the initial conditions previous defined. kOmegaSST turbulence model has a precise formulation and uses the standard k-ω model in the inner part of the boundary layer. The notation ω is the specific dissipation rate. To solve the boundary layer near to the hull the flow, in these zones, is modeled by empirical wall function. The values for the turbulent kinetic energy and dissipation ratio are k=0.00015 [m²/s²] and ω=2 [1/s], respectively. These values were estimated by:

$$k = \frac{1}{2}\overline{U' \cdot U'} = \frac{1}{2}\left(U_x'^2 + U_y'^2 + U_z'^2\right) \tag{14}$$

$$\omega = \frac{\sqrt{k}}{l \sqrt[4]{C_\mu}} \tag{15}$$

Due to this, the percentage of the turbulence intensity and the turbulence length scale for the DTC hull can be calculated by, respectively:

$$I\% = 100\sqrt{\frac{2}{3}\frac{k}{U^2}} = 100\sqrt{\frac{2}{3}\frac{(0.00015)}{1.668^2}} = 0.6$$
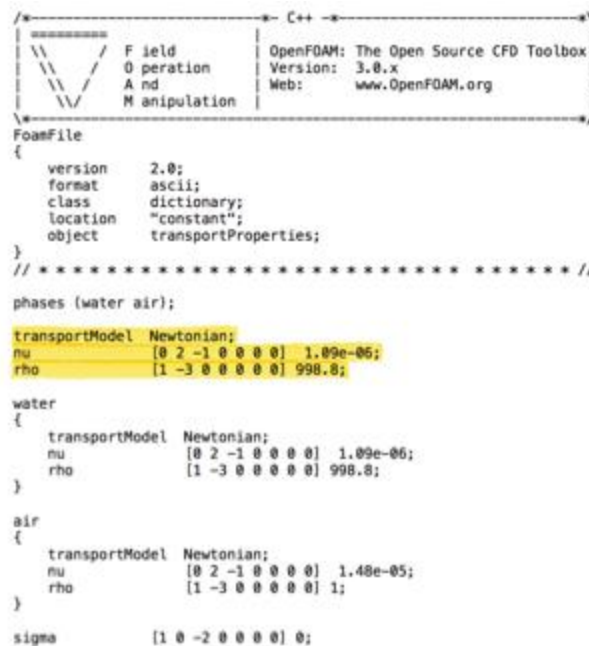
$$l = \frac{\sqrt{k}}{\omega \sqrt[4]{C_\mu}} = \frac{\sqrt{0.00015}}{2\sqrt[4]{0.09}} = 0.0112 \ [m]$$

y+ is the non dimensional distance and OpenFOAM is a post processing tool applied to near-wall cells of all wall patches. The value obtained by y+ can describe the places where the mesh has to have more number of cells. y+ is defined by:

$$y^+ = \frac{u_* y}{\nu} \tag{16}$$

Where u_* is the frictional velocity at the nearest wall, y is the distance to the nearest wall and ν is the local kinematic viscosity of the fluid. To calculate y+ the Transport Properties file was modified as the Figure 22.

Figure 22: Transport Properties file modification

2.2.6 Solver Setup

In the DTC Hull resistance case, the InterFoam solver for multiphase flow is used. OpenFOAM used *fvSchemes* file, where is set the solution method of

solution. Inside this file are terms that include derivatives and interpolations that require numerical schemes to discretize the RANS equations and others. Table 10 describes the schemes of solution into this file:

Table 10: Numerical Schemes

Term	Variable	Scheme	Description
Time	Default	localEuler	Local time step, first order, bounded, implicit
Gradient	Default	Gauss linear	Second order, linear interpolation
Divergence	Div(rho*phi,U)	Gauss linear upwind	Second order, linear interpolation, upwind differencing
Laplacian	Default	Gauss linear corrected	Second order, linear interpolation, unbounded and conservative
Interpolation	Default	Linear	Linear interpolation
snGradient	Default	Corrected	Explicit non-orthogonal correction
Flux	P_rgh, pcorr, alpha1	-	Flux generated for these fields

fvSolution specifies how the discretized equations are solved. In this file, the solver tolerance is specified for each variable, as shown in Table 11.

Table 11: Solvers set up in fvSolution

Variable	Solver
alpha.water	smoothSolver
pcorr	GaussSeidel
p_rgh	GAMG
p_rghFinal	GAMG
U|k|omega	smoothSolver

2.2.7 Parallels Performance and Scalability

The solution of the problem can be performed using several CPUs. *descomposeParDict* directory divide the computational domain, to process the information in a more efficient way. In this file the first entry is the number of sub-domains, which the case will be decomposed, or the number of processors. This decomposition can be done using a weight factor for each processor. The method of decomposition is SCOTCH, which requires a no-geometric input from the user and tries to minimize the number of processor boundaries.

Scalability is the capacity of the processor to handle a growing amount of work [14] and it is shown using the timing and performance of different runs using the same mesh and changing the numbers of processors. Table 12 describes computational resources used in this project using the default mesh provided by OpenFOAM.

Table 12: Workstation Description

Maker	DELL Precision T7610
Software	Red Hat Enterprise Linux Workstation 7.2
Memory	31.2 GiB
Processor	Intel® Xeon(R) CPU E5-2630 v2 @ 2.60GHz x 24
OS Type	64 bit
Graphics	Quadro K4000/PCIe/SSE2
GNOME	Version 3.14.2

By default, DTC Hull case was set up to use 8 processors. But to understand the speedup behavior, additional simulations using different number of processor were performed. Speedup for p processors is defined as:

$$Speedup = \frac{\text{time for 1 processor}}{\text{time for } p \text{ processors}} \tag{17}$$

The number of processors was set up according the maximum number of processors available in the Workstation. Table 13 shows the time that takes InterFoam to solve 4000 seconds or time steps, and the speedup.

Table 13: DTC Hull case Speedup

N° Processors	SpeedUp	Solving Time of InterFOAM [h]
1	1	5.60
2	1.05	5.33
4	1.42	3.96
8	1.92	2.91
12	**2.05**	**2.74**
16	1.92	2.91
24	1.52	3.68

Figure 23 presents the speedup curve, where highest peak of the curve is for 12 processors running in parallel. But despite this, the following runs were run with 8 processors because the difference in working time is small.

In this case the system requires more time to share all information between each other. This increase the time of resolution for that specific mesh density (848,025 cells). For other meshes with more number of cells it would be necessary to use more processors to decrease the time of resolution.

Figure 23:DTC Hull Speedup curve

SpeedUp
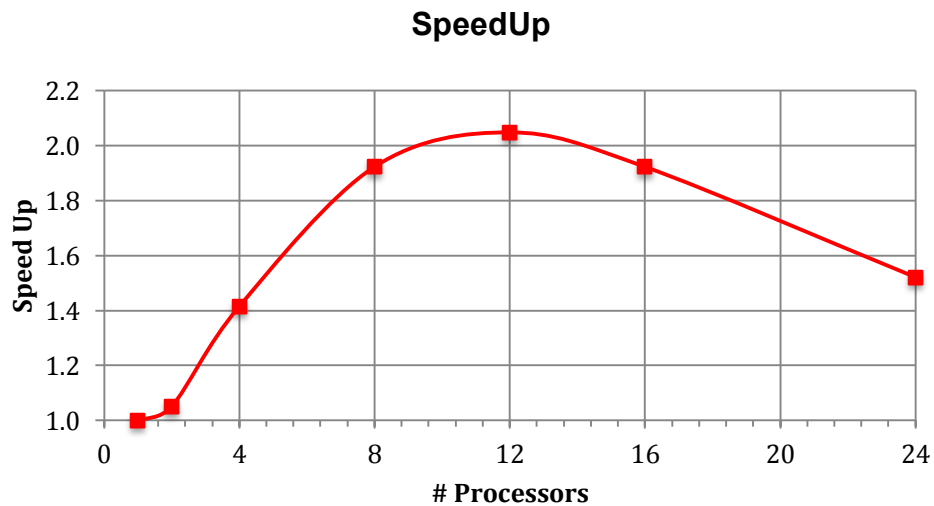
2.2.8 Mesh Convergence

Discretization errors are proportional to cell size. It is expected that increasing the number of cells will decrease the discretization error. However, this is not always true. To assess this, a mesh convergence study is done. Using the same number of processors and changing the mesh of DTC Hull case.

Table 14: Mesh Properties for DTC Hull case with 12 processors

N°	Mesh Number of Cells	InterFoam Solve Time [h]
Coarse-DTCMesh1	220,563	0.53
Medium-DTCMesh2	450,140	1.34
Tutorial-DTCMesh3	848,025	2.74

Figures 24 to 32 shows different mesh generation in x, y and z planes.

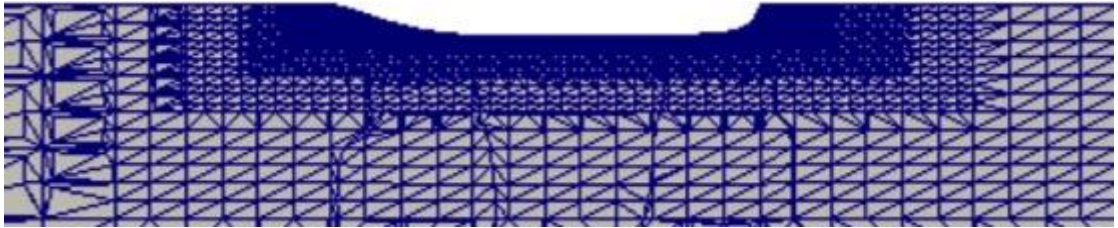**Figure 24:** X Plane DTCMesh1 Projection

Figure 25: X Plane DTCMesh2 Projection
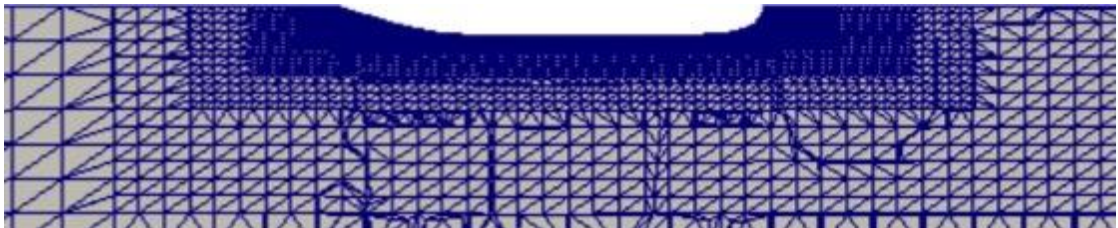
Figure 26: X Plane DTCMesh3 Projection
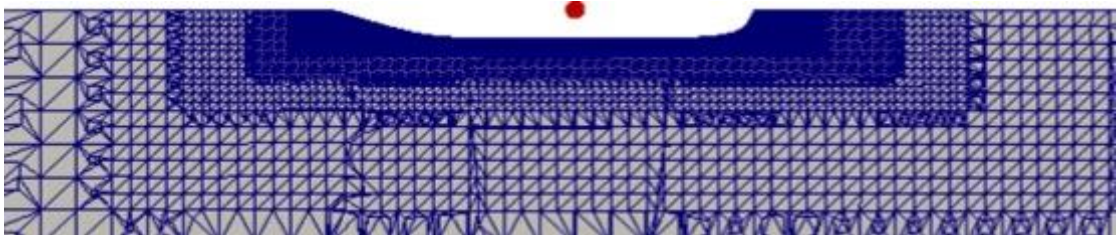
Figure 27: Y Plane DTCMesh1 Projection
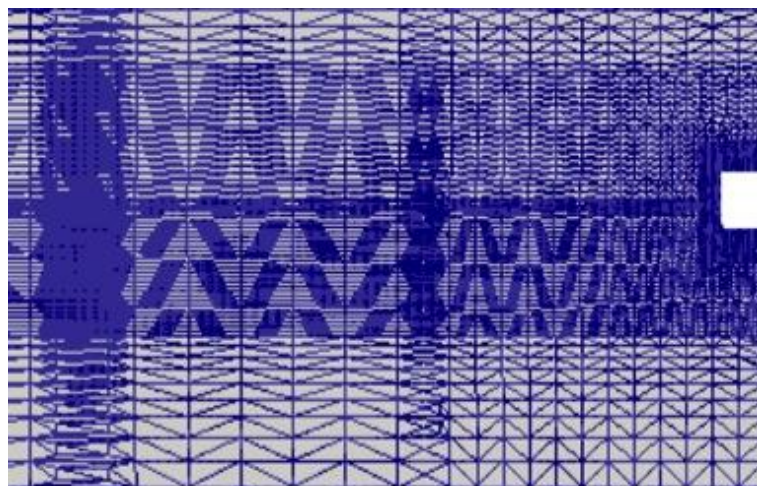
Figure 28: Y Plane DTCMesh2 Projection
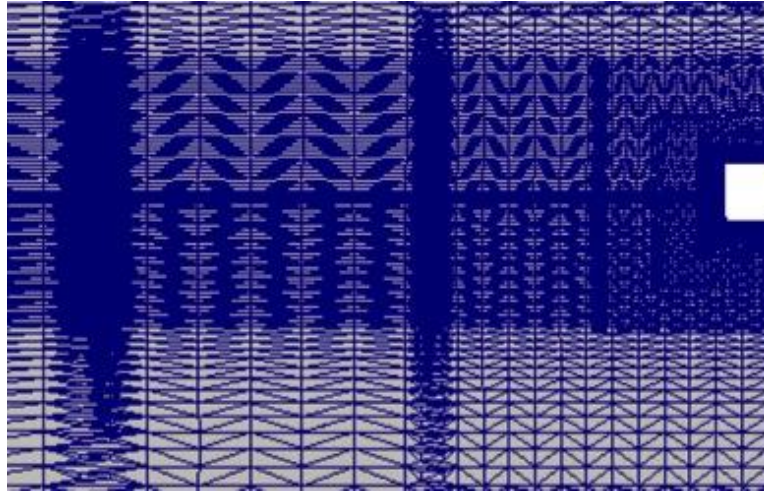
Figure 29: Y Plane DTCMesh3 Projection
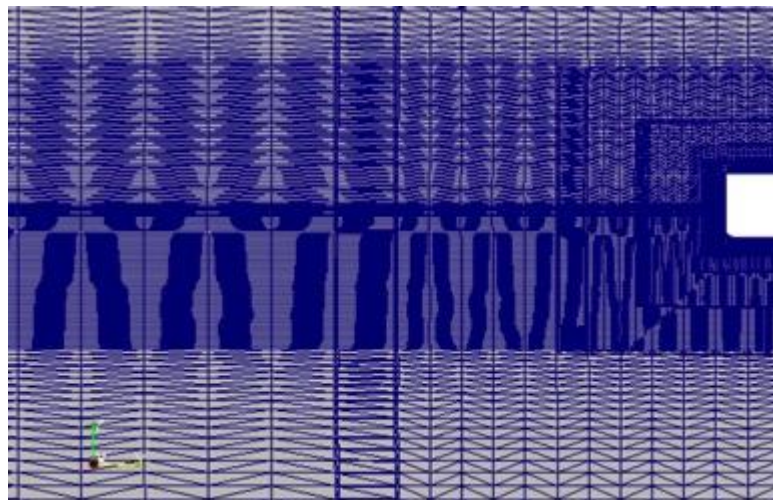
Figure 30: Z Plane DTCMesh1 Projection
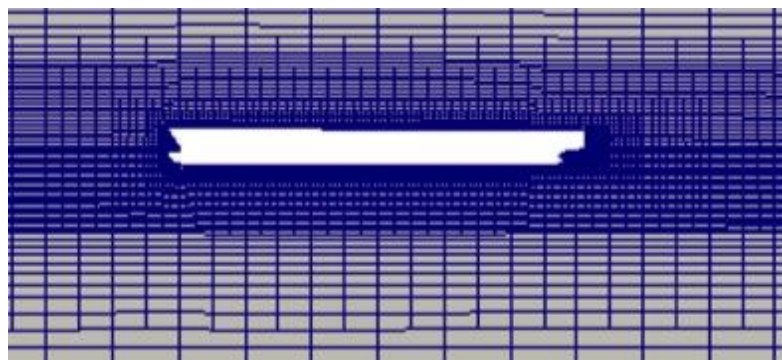
Figure 31: Z Plane DTCMesh2 Projection
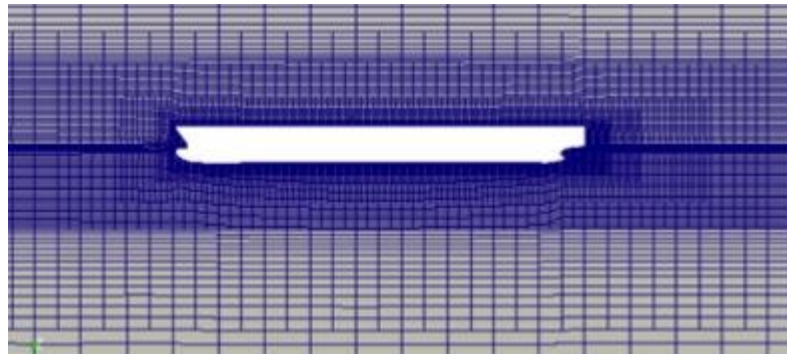
Figure 32: Z Plane DTCMesh3 Projection
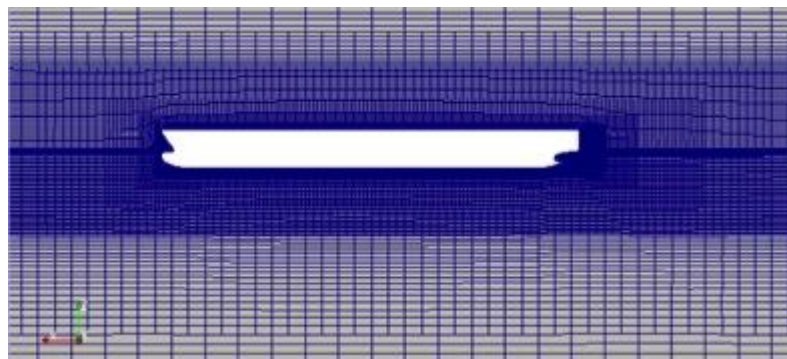
The value of y+ is used as a way to visualize the distribution of cells around the hull and check the quality of the mesh that captures the boundary layer developed. The range of y+ has to be 30<y+<100 [11]. Figures 33 to 35 show the y+ distribution around the DTC Hull for three different meshes after 4000 iterations. y+ was calculated only for one fluid, fresh water, for this reason only the wetted area is considering as reliable.

Figure 33: y+ for DTCMesh1 at time 4000 [s]
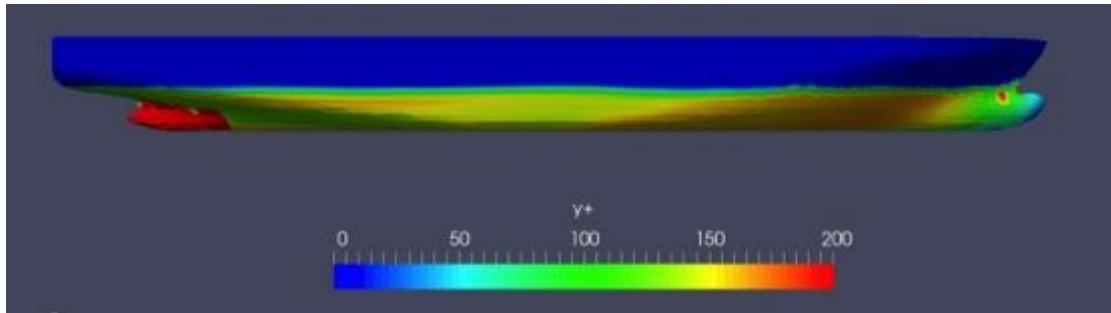
Figure 34: y+ for DTCMesh2 at time 4000 [s]
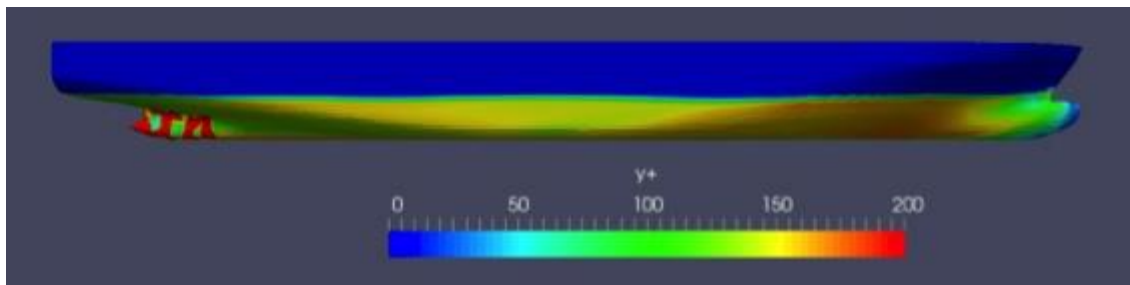
Figure 35: y+ for DTCMesh3 at time 4000 [s]
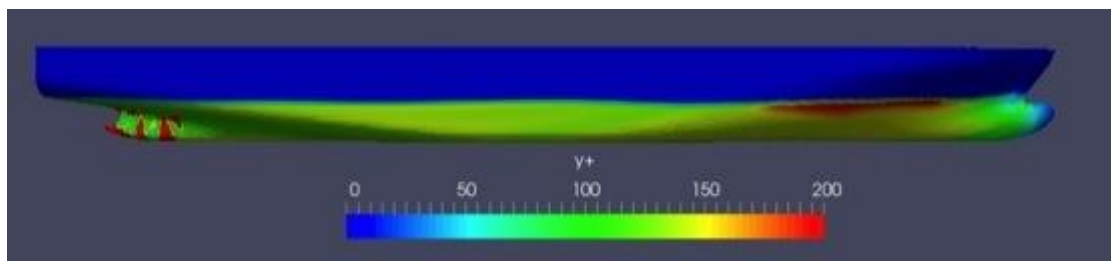
2.2.9 Resistance Results

The numerical resistance results obtained in this work were compared to the experimental results published by Moctar, Shigunov & Zorn [9] where the model was allowed to sink and trim. Table 15 shown the results of resistance model test at different Froude numbers.

Table 15: Results of resistance model tests

v_{Model} [m/s]	Fn	Re x 10^{-6}	R_T [N]	C_T x 10^3
1.335	0.174	7.319	20.34	3.661
1.401	0.183	7.681	22.06	3.605
1.469	0.192	8.054	24.14	3.588
1.535	0.200	8.415	26.46	3.602
1.602	0209	8.783	28.99	3.623
1.668	0.218	9.145	31.83	3.670

Source: Moctar, Shigunov & Zorn [8]

Where Froude and Reynolds number are defined as:

$$F_n = \frac{V}{\sqrt{g\,L}} \tag{18}$$

$$R_e = \frac{V\,L}{\nu} \tag{19}$$

Where V is the ship velocity in meters per second, g the gravity in meter per square second, L the length between perpendiculars of the ship in meters and ν the cinematic viscosity of the fluid in square meters per second.

It is required to modify *controlDict* file to report the forces due to resistance for the hull in directions *x, y* and z, and save the results in a file. The resistance estimated by OpenFOAM has two components: pressure force and viscous force. Figure 36 shows these two components and the total resistance at Fn=0.218.

Also, the file controlDict was modified to obtain residuals of dynamic pressure (p_rgh), VoF (alpha.water), specific dissipation rate (ω or omega) and turbulent kinetic energy (k), as shown in Figure 37.

Figure 36: Resistance components at Fn=0.218
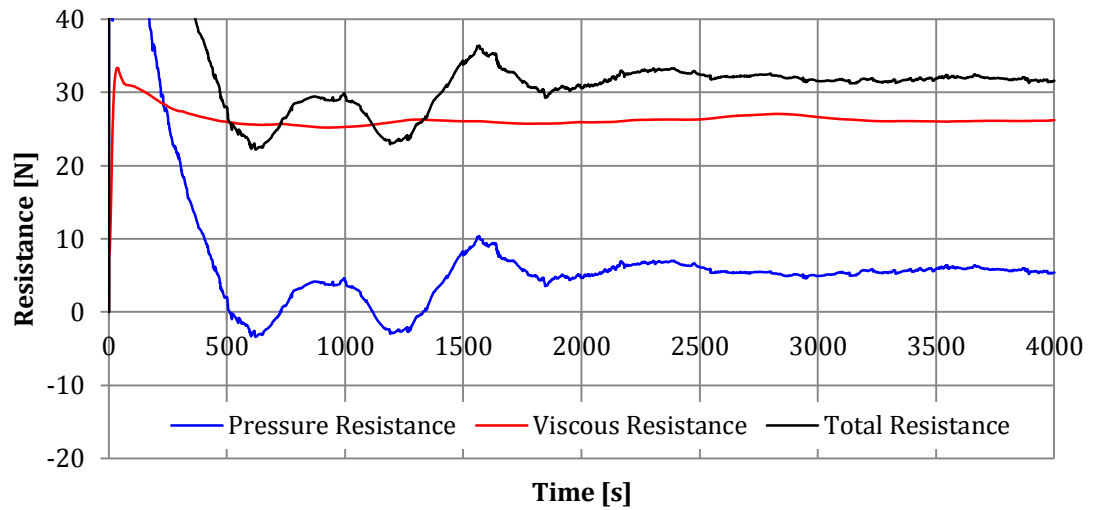
Figure 37: ContoDict file modification

```
functions
{
    forces
    {
        type forces;
        functionObjectLibs ( "libforces.so" );
        patches (hull);
        rhoInf  998.8;
        rhoName rho;
        UName   U;
        log     on;
        outputControl   timeStep;
        outputInterval  1;
        CofR (0.9348 0 0.08);
    }
     residuals
    {
        type residuals;
        functionObjectLibs ("libutilityFunctionObjects.so");
        outputControl timeStep;
        outputInterval 1;
        fields
        (
            alpha.water
            p_rgh
            omega
            k
        );
    }
}
```

Figures 38 to 41 shows residuals of the variables setting before at a Froude
number of Fn=0.218.

Figure 38: DTC Hull Alpha.water residuals at Fn=0.218
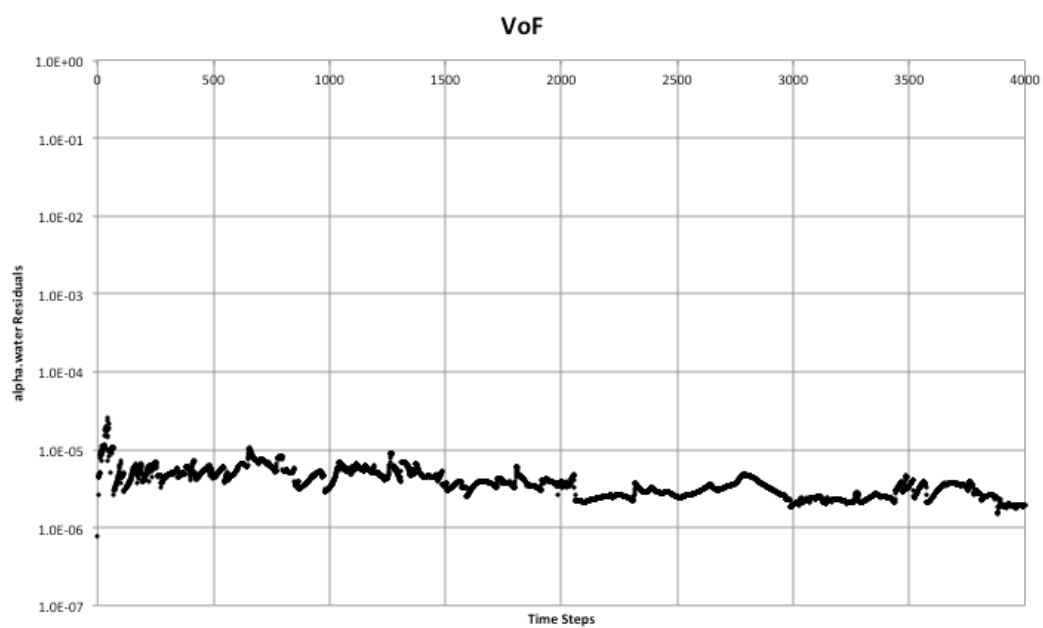
Figure 39: DTC Hull Dynamic pressure residuals at Fn=0.218
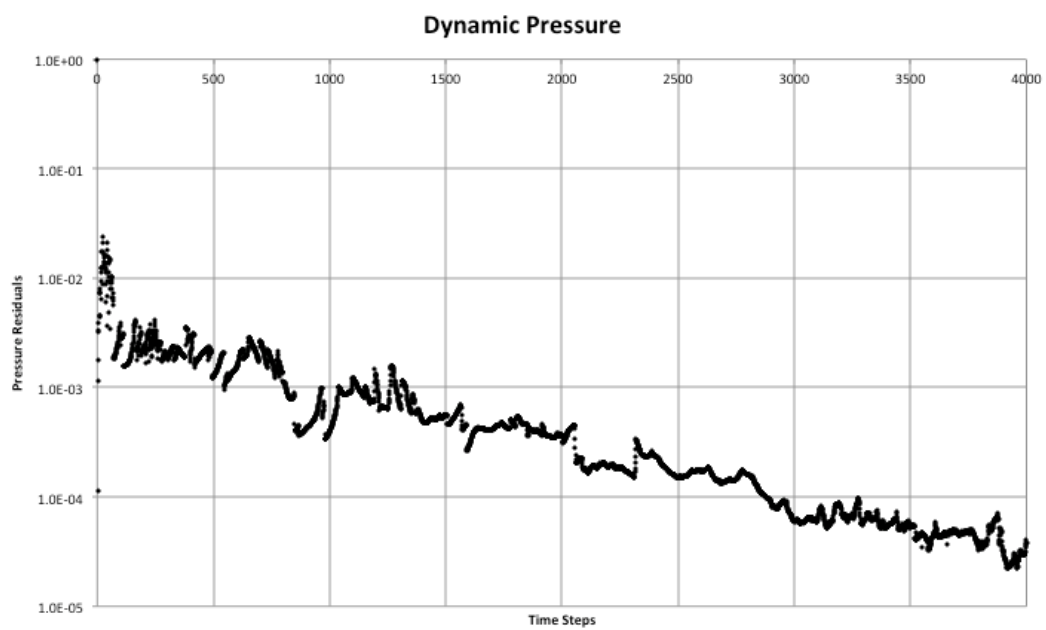
Figure 40: DTC Hull Dissipation rate residuals at Fn=0.218
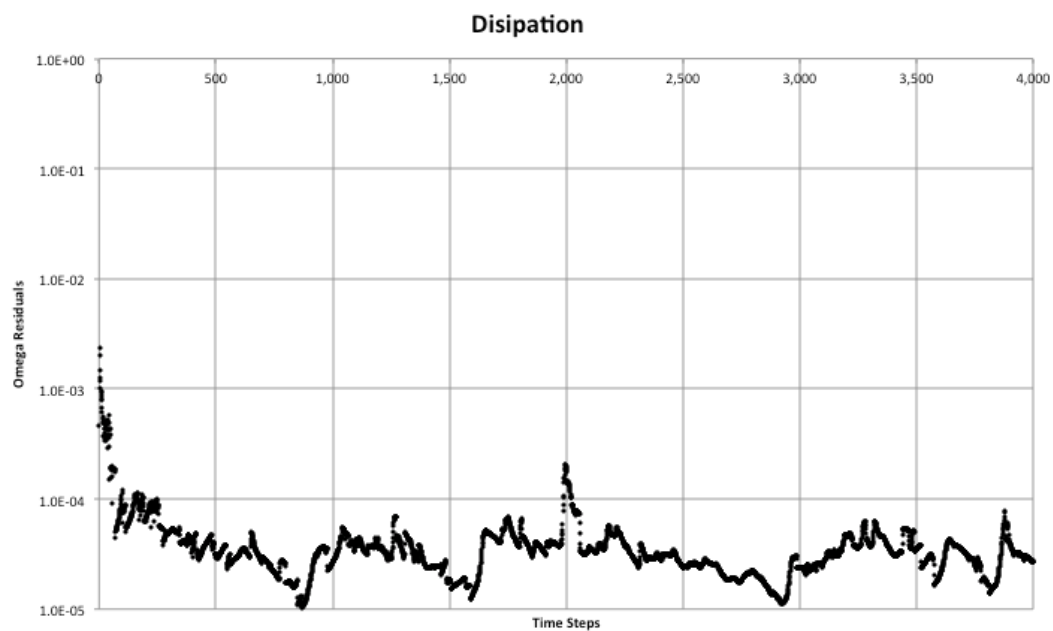
Figure 41: DTC Hull Turbulent kinetic energy residuals at Fn=0.218
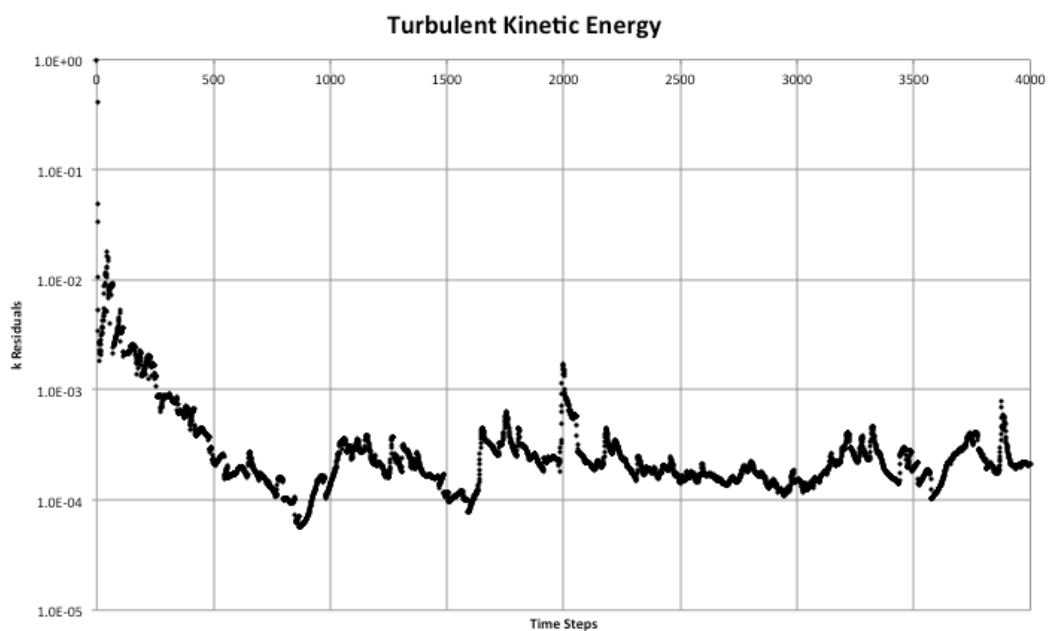
At a Froude number of 0.218, interFoam solver was run using three different meshes. Table 16 shows the number of cells per processor, using 12 processors by each type of mesh, and the total of cells.

Table 16: Total of cells per processor

|		Coarse DTCMesh1	Medium DTCMesh2	Tutorial DTCMesh3
Processors	**0**	18,563	37,156	70,317
	1	18,289	37,867	70,854
	2	18,287	37,137	70,109
	3	18,563	37,880	71,374
	4	18,563	37,886	71,264
	5	18,563	37,885	71,374
	6	18,197	37,838	71,374
	7	18,396	37,145	70,127
	8	18,242	37,508	70,720
	9	18,245	37,150	69,962
	10	18,198	37,455	69,980
	11	18,457	37,233	70,570
TOTAL OF CELLS		**220,563**	**450,140**	**848,025**

Figure 42 represent the resistance time history for different meshes, contrasting with the experimental result at Fr=0.218 of 31.83 [N]. Finer mesh converges after 3000 seconds in the case of tutorial. It is expected that the coarser meshes needs more run time to converge, because it still has oscillations.

The error is calculated using the following formula:

$$error = \frac{R_{t\,OpenFOAM} - R_{t\,experimental}}{R_{t\,experimental}} \qquad (20)$$

Table 17 represents the errors between numerical average results of the three last 500 steps of time meshes with respect to experimental results.

Figure 42: DTC Meshes Convergence of total Resistance using interFOAM solver at Fr=0.218
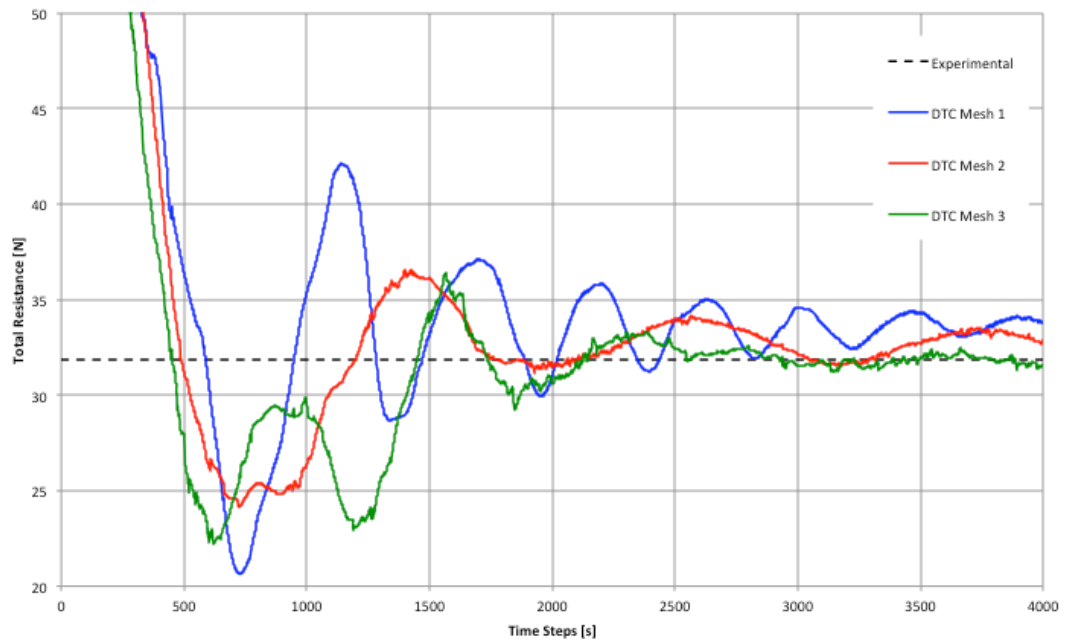
Table 17: Numerical Resistance Error for different Meshes

Coarse Mesh	Medium Mesh	Tutorial Mesh
5.88%	4.11%	0.25%

Finally, the Tutorial Mesh is used for the following simulations with different velocities considering the error from the different meshes.

Resistance using interDyMFOAM

interDyMFOAM solver was used in DTC case. The principal difference between interFOAM and interDyMFOAM is the mesh. interDyMFOAM have a dynamic mesh given their cells an automatic motion. And also, for DTC case,

the model has 2 degrees of freedom: Heave and Pitch. Figure 43 shows the

six degrees of freedom of a rigid body.

Figure 43: Six degrees of freedom of a system
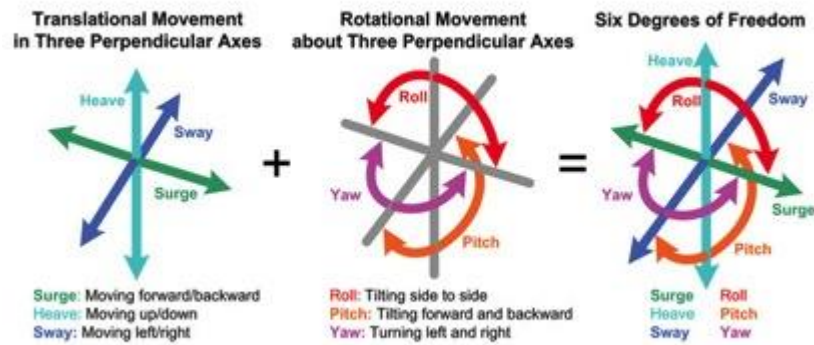
Source: Nelson [14]

Dynamic mesh is setting on constant directory. Centre of mass can be

estimated using Rhinoceros analyze tool, mass properties/area centroid. Due

the symmetry of the domain, only haft of the hull mass is considerate. The

moment of inertia can be estimated using the followings formula [16]:

$$I_{xx} = (35\% * B)^2 * M \tag{21}$$

$$I_{yy} = (25\% * L_{wl})^2 * M \tag{22}$$

$$I_{zz} = (25\% * L_{wl})^2 * M \tag{23}$$

Where I is the inertia in the three directions, M is the mass, B the beam and

L_{wl} is the length at the water line. Figure 44 shows the text file with the other

required data.

Figure 44: DTC Hull dynamic mesh file for InterDyMFOAM solver

```
dynamicFvMesh          dynamicMotionSolverFvMesh;

motionSolverLibs       ("libsixDoFRigidBodyMotion.so");

solver                 sixDoFRigidBodyMotion;

sixDoFRigidBodyMotionCoeffs
{
    patches         (hull);
    innerDistance   0.3;
    outerDistance   1;

    centreOfMass    (2.929541 0 0.2);
    mass            412.73;
    momentOfInertia (40 921 921);
    rhoInf          1;
    report          on;

    value           uniform (0 0 0);

    accelerationRelaxation 0.4;

    solver
    {
        type Newmark;
    }

    constraints
    {
        zAxis
        {
            sixDoFRigidBodyMotionConstraint line;
            direction       (0 0 1);
        }
        yPlane
        {
            sixDoFRigidBodyMotionConstraint axis;
            axis            (0 1 0);
        }
    }

    restraints
    {
        translationDamper
        {
            sixDoFRigidBodyMotionRestraint linearDamper;
            coeff           8596;
        }
        rotationDamper
        {
            sixDoFRigidBodyMotionRestraint sphericalAngularDamper;
            coeff           11586;
        }
```

interFOAM and interDyMFOAM solvers were compared at different velocities with their respective experimental results. With this comparison may see the difference between these two solvers and the experimental results. Figures 45 to 49 are the total resistance over the time for interFOAM and interDyMFOAM, at different Froude numbers.

Figure 45: Total resistance over the time with different solvers at Fn=0.174
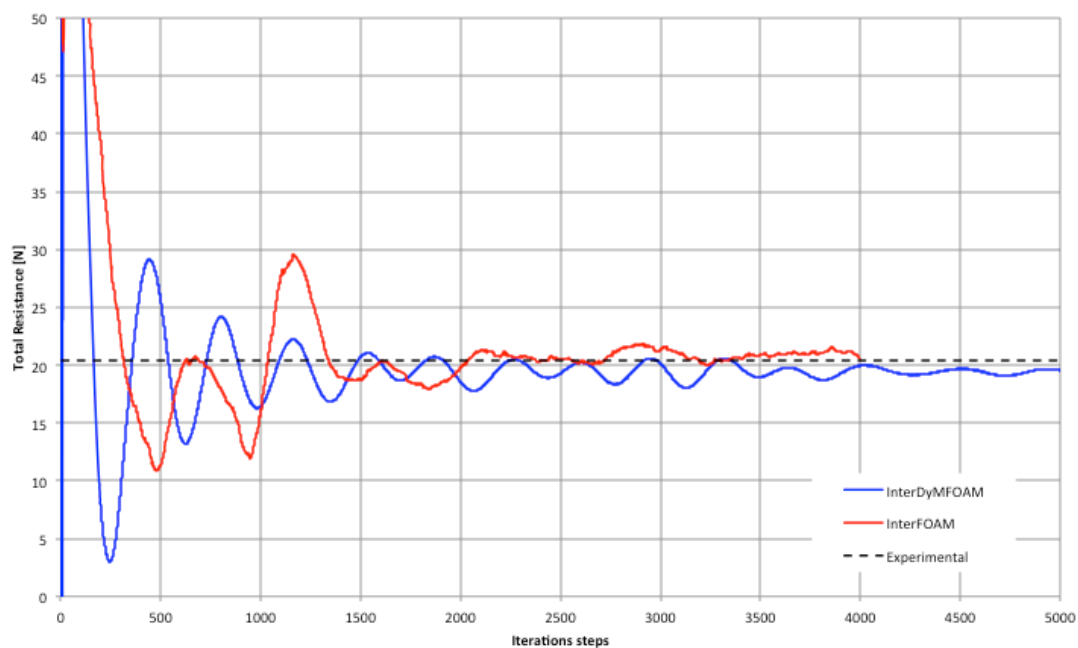
Figure 46: Total resistance over the time with different solvers at Fn=0.183
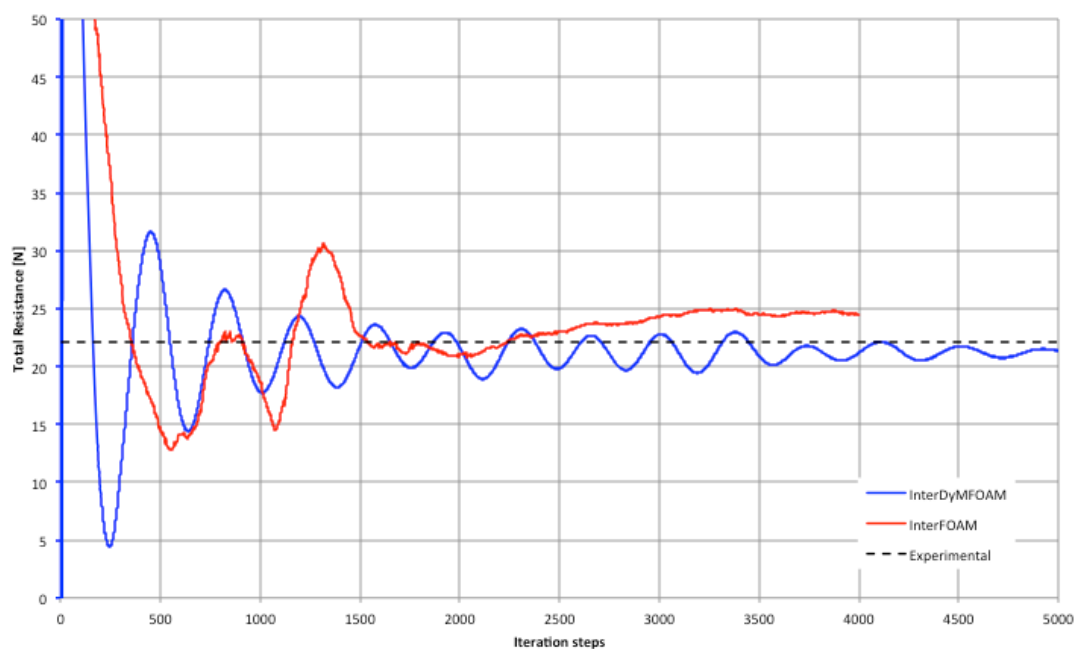
Figure 47: Total resistance over the time with different solvers at Fn=0.192
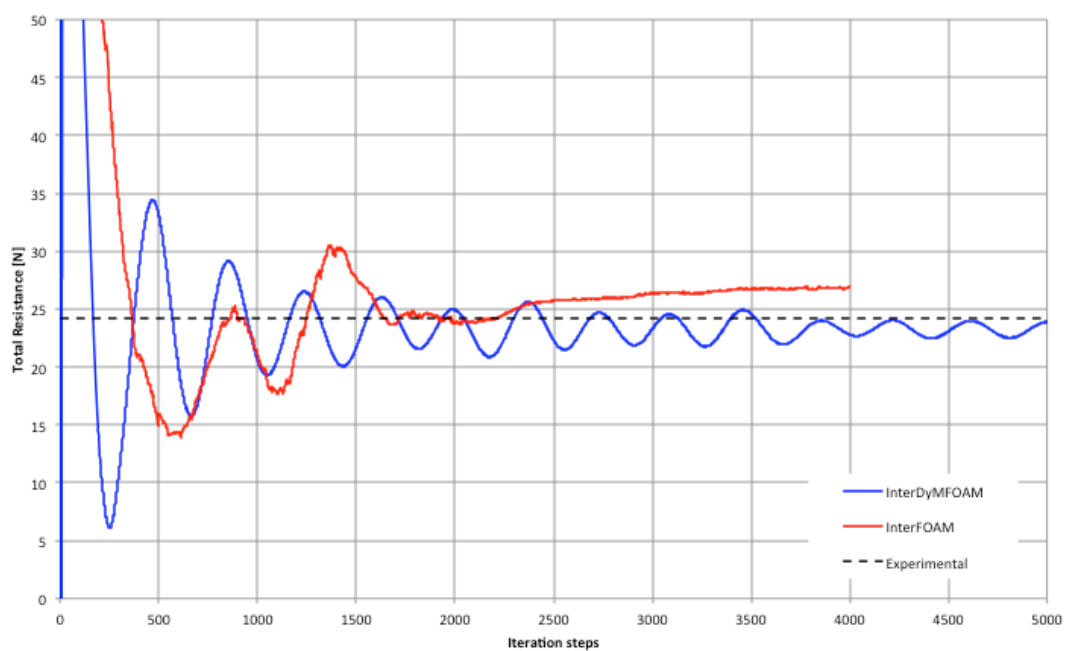
Figure 48: Total resistance over the time with different solvers at Fn=0.200
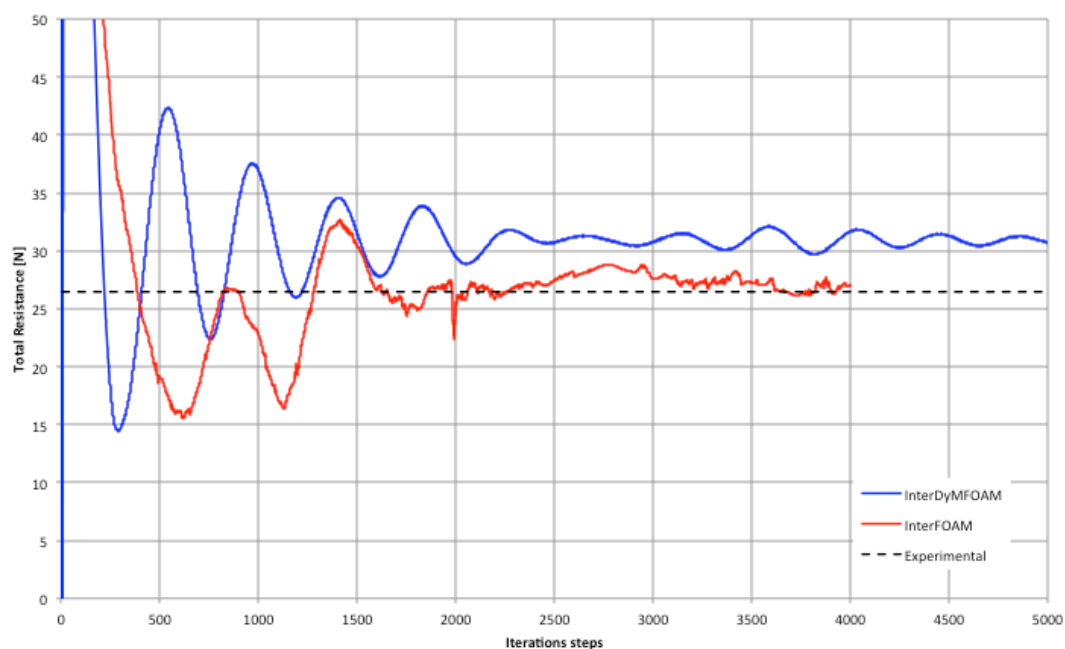
Figure 49: Total resistance over the time with different solvers at Fn=0.218
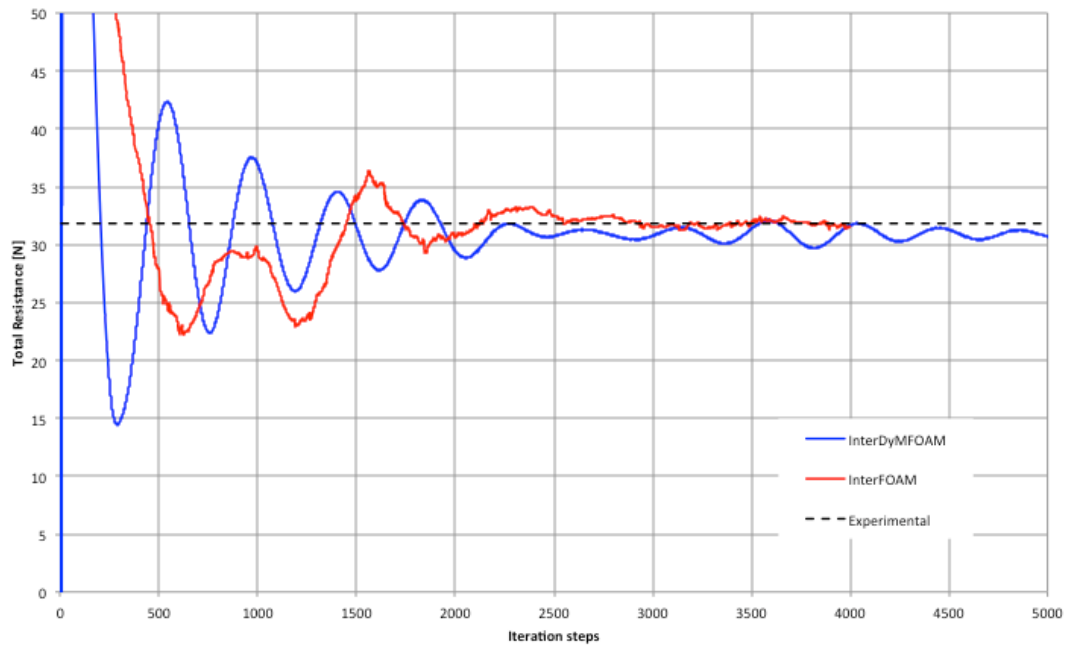
To compare with the experimental results, DTC Hull case was run at different Froude numbers. Table 18 shows the results of model test and numerical simulation using interFoam, as static method, and interDyMFOAM, as a dynamic method.

Table 18: DTC Hull case resistance for different number of Froude

Fn	Exp.	interFOAM R_t [N]	interDyMFOAM R_t [N]	interFOAM Error	interDyMFOAM Error
0.174	20.34	21.03	19.41	3.40%	4.59%
0.183	22.06	24.56	21.17	11.35%	4.02%
0.192	24.14	26.78	23.35	10.94%	3.29%
0.200	26.46	26.77	25.42	1.17%	3.92%
0.218	31.83	31.91	30.84	0.25%	3.12%
			Average	5.42%	3.79%

Figure 50: Total Resistance of DTC at different Froude Number and Solvers
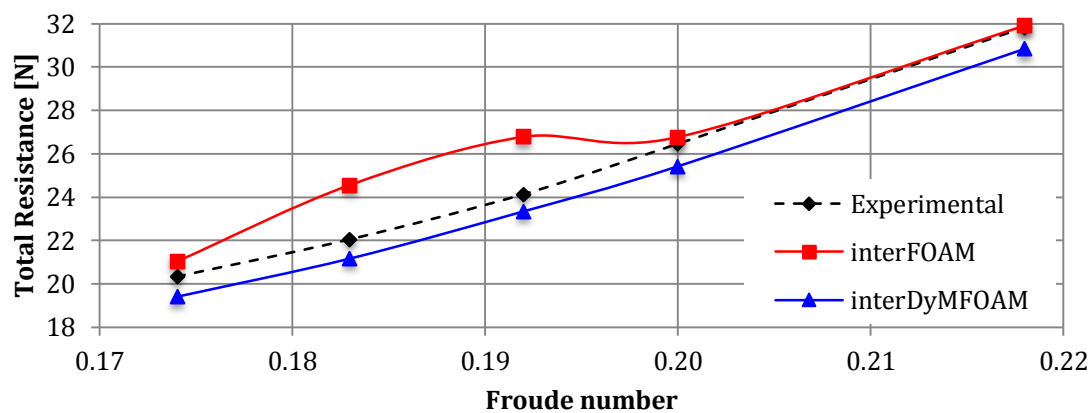
InterDyMFOAM results are closer to experimental data, maybe because the model allowed sinking and trimming in the experiments; the same configuration did it by interDyMFOAM.

Figure 51 represents the free vertical translation of the ship (sinkage z) as a percentage of perpendicular length at different Froude numbers.

Figure 51: DoF, vertical translation for DTC hull at different Froude numbers

Sinkage
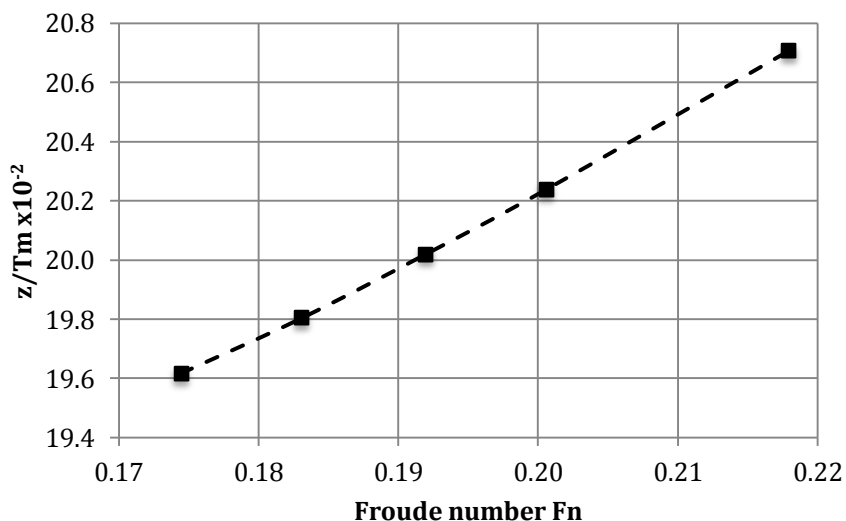
Figure 52 shows the trimming angle at different Froude numbers, the free longitudinal rotation.

Figure 52: DoF, trim for DTC hull at different Froude numbers

Trim
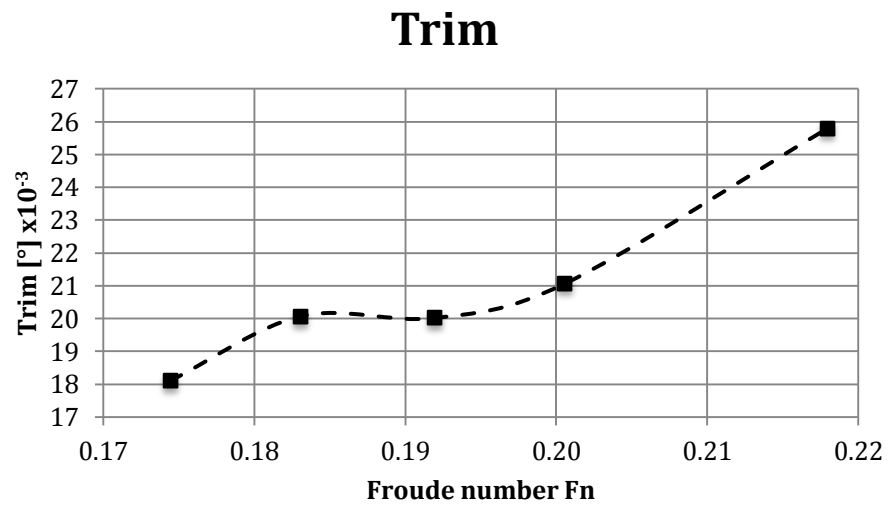
CHAPTER 3

CATAMARAN RESISTANCE

In this chapter, the catamaran hull resistance is estimated using InterFOAM solver. First, a 3D model was generated with a STL extension. The boundary and initials conditions were set up following DTC case. A mesh convergence study was developed for a demi-hull in light condition at minimum velocity. Three models with different mesh density were implemented for this study. Finally, the ship resistance was calculated for demi and twin hulls, following the velocity and load conditions setting in experimental data [1].

3.1 3D GENERATION MODEL

The geometry of Catamaran was taken from Chávez and Lucín previous work [1]. The 3D surface model was generated with the body and profile plan in Computer Aided Design (CAD) software Rhinoceros 3D [17] and positioned the after perpendicular line at the origin axes before exporting as STL file to import into the CFD code, OpenFOAM. Figure 53 shows the 3D Rhinoceros scaled demi-hull model.

Figure 54 shows the scale model of catamaran used in experimental test described in Figure 4.

Figure 53: Scale Catamaran 3D Model used in the CFD simulations
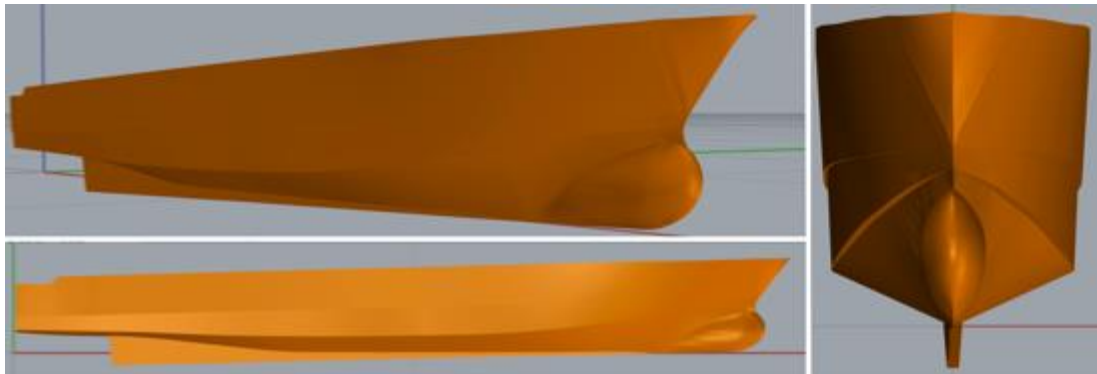
Figure 54: Photographs of real scale Catamaran model used for experimental tests
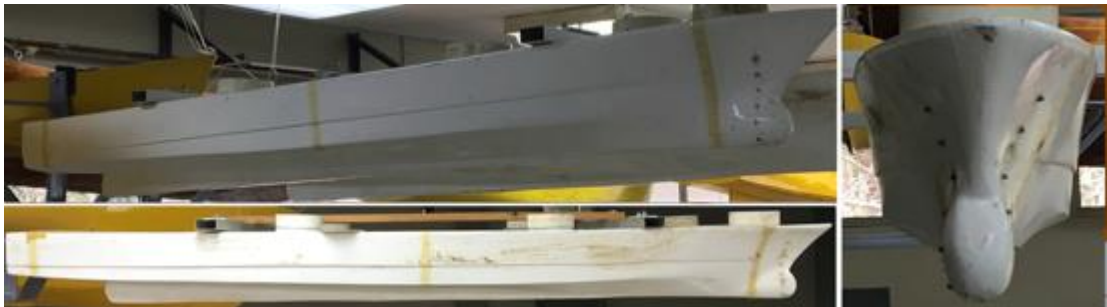
3.2 BOUNDARY AND INITIAL CONDITIONS

The computational domain was build as a rectangular block around the hull (demi and twin hulls) following the proportions expressed before for DTC case in deep water; Figure 55 shows the principal dimensions in meters.

The initials conditions were set in *0.org* directory, where the speed was changed following experimental tests, see Table 19. The others initial conditions, as dissipation (omega), turbulent cinematic viscosity (nut), turbulent kinetic energy (k) and dynamic pressure (p_rgh), were setting as the DTC case.

Figure 55: Catamaran domain size
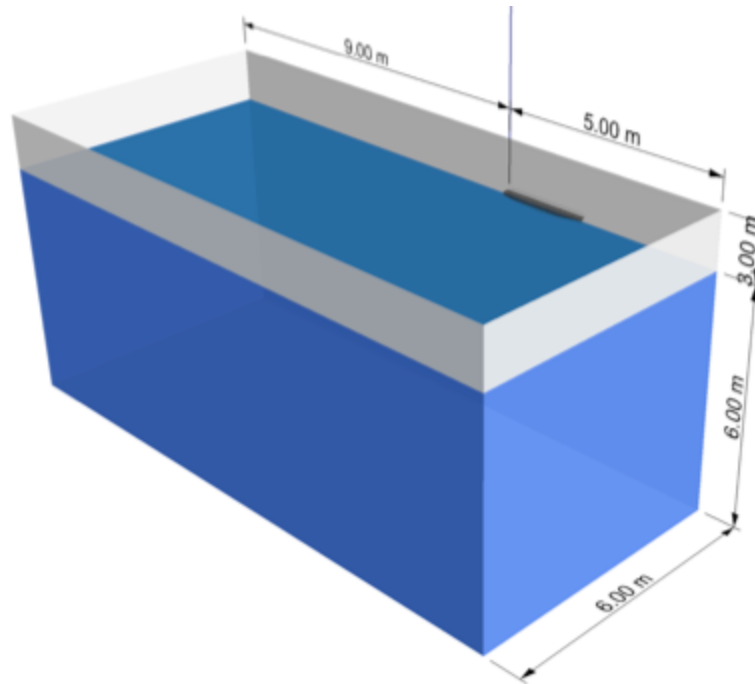
Table 19: Velocities for Catamaran Different cases of Load Condition

Light Condition Velocities [m/s]		Full Condition Velocities [m/s]	
Demi-hull	Twin-hull	Demi-hull	Twin-hull
1.05	1.05	1.03	1.05
1.14	1.14	1.10	1.12
1.20	1.26	1.23	1.25
1.30	1.32	1.35	1.33
1.45	1.47	1.45	1.46
-	1.53	-	1.55
-	1.76	-	1.75
-	1.94	-	-

Catamaran test matrix has a total of 25 simulations, where the Draft for Light and Full Load Conditions are 0.086 [m] and 0.103 [m], respectively.

3.3 MESH CONVERGENCE STUDY

To identify the mesh density needed for the Catamaran cases a mesh convergence study was perform. The domain was divided into six blocks with different mesh densities. At first, a medium mesh was set up following the same division of the coordinate axes used in the DTC case. From this point, a coarse and fine mesh was created for the study. Table 20 shows the number of cells for each mesh.

Table 20: Number of cells by each type of mesh

Type of Mesh	No. of Cells
Coarse - Mesh1	250,599
Medium - Mesh2	1'000,278
Fine - Mesh3	1'566,579

To visualize the convergence of the simulations, Figure 56 shows the force time history (4,000 seconds) for each mesh.

Figure 56: Total Resistance along the setting time of convergence for different mesh densities, Light Condition at V=1.05 [m/s]
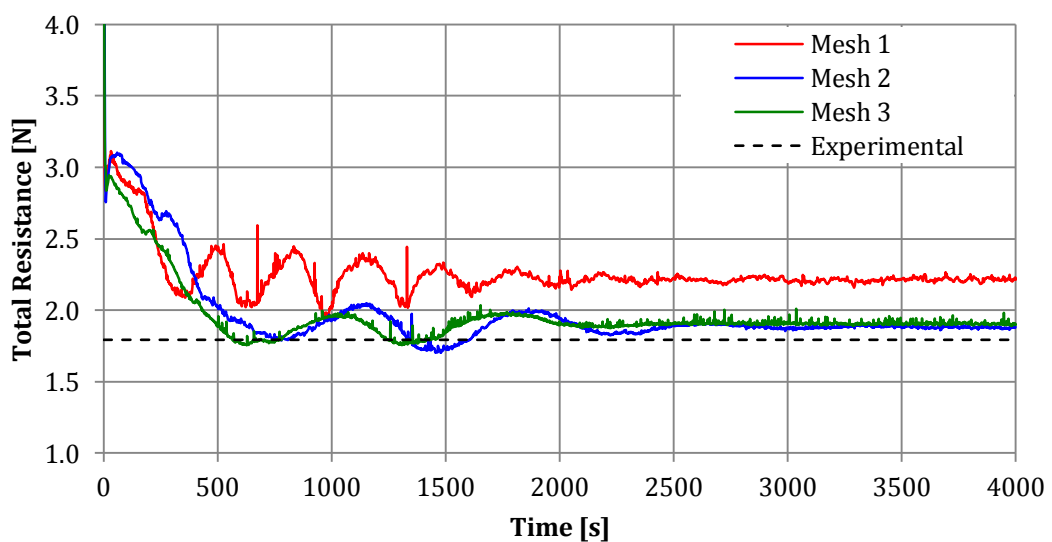
Four thousand values of resistance were generated at the Light Load condition at v=1.05 [m/s]. Table 21 shows the average of the last five hundred values for the resistance of each mesh and its error when compared with an experimental value of $R_{t\,exp}$=1.79 [N].

Table 21: Total Resistance and Errors for 3 types of meshes

	Resistance Average	% Error	Standard Deviation
Mesh 1	2.22	24%	0.71
Mesh 2	**1.88**	**5%**	**0.34**
Mesh 3	1.91	6%	0.50

The errors between meshes 2 and 3 are closer. But, analyzing the standard deviation, Mesh 2 has less variation of resistance in the analyzed steps. Mesh 2 was selected to set up the other simulations. Figure 57 to 60 represent the mesh 2 configuration around the hull and the 3 coordinates plans slides.

The residuals of dynamic pressure (p), dissipation rate (omega), VoF (alpha.water) and turbulent kinetic energy (k) were plotted to check the convergence of Mesh 2, see Figure 61 to 64.

Figure 57: Catamaran Mesh 2
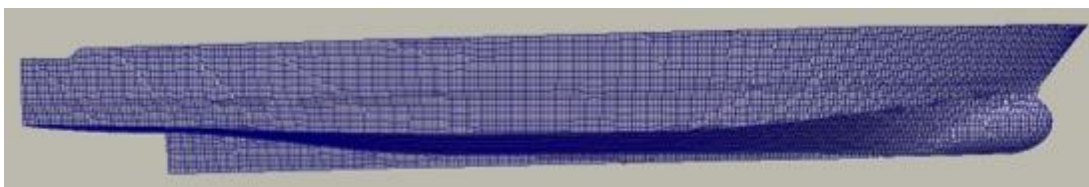
Figure 58: Y Plane Mesh 2 Projection
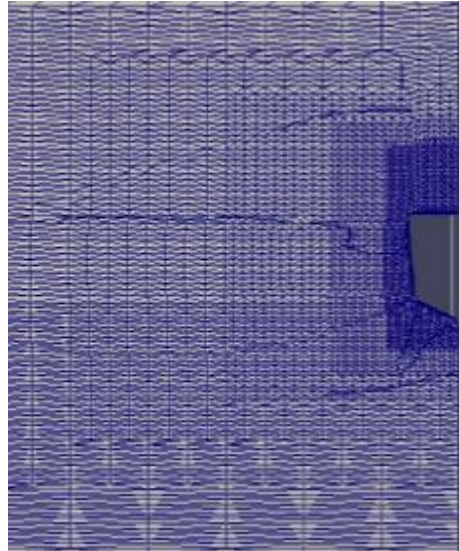
Figure 59: X Plane Mesh 2 Projection
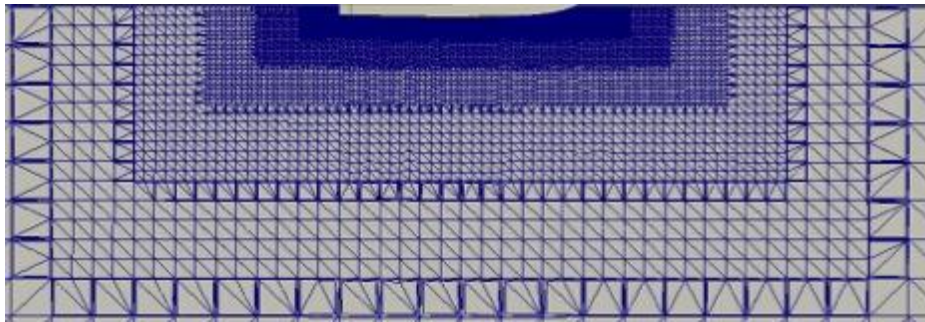
Figure 60: Z Plane Mesh 2 Projection
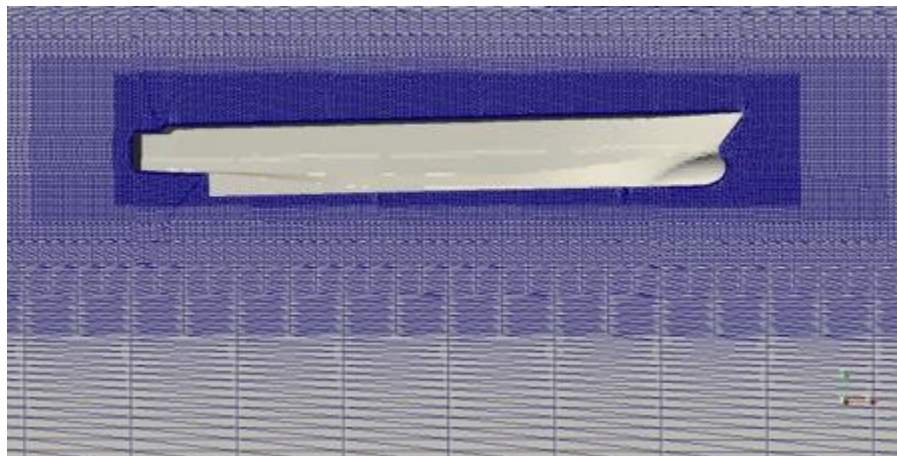
Figure 61: Catamaran Hull Alpha.water residuals at Fn=0.2453
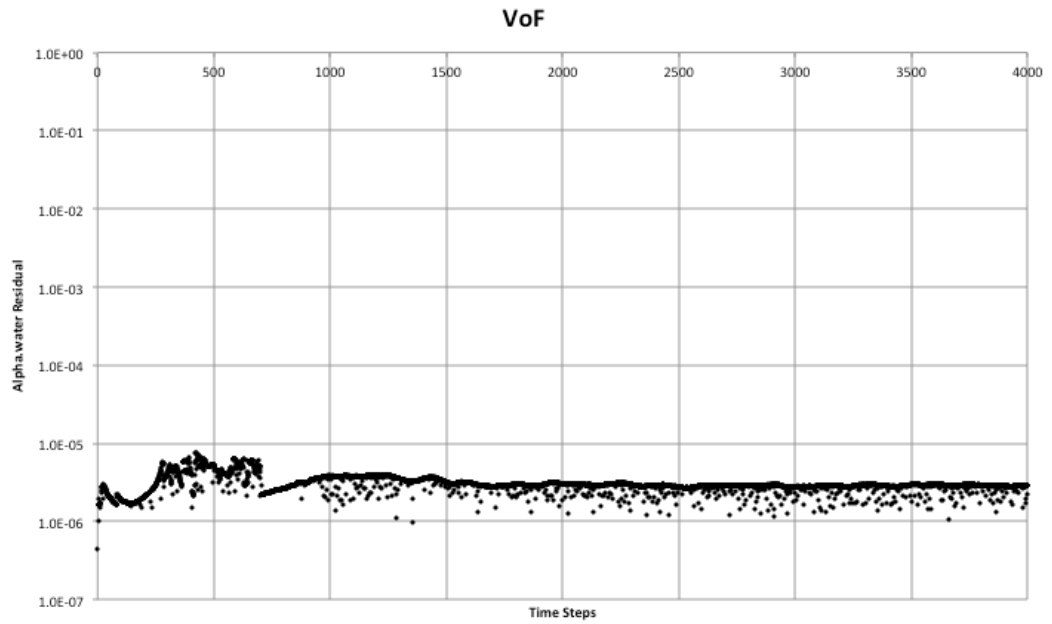
Figure 62: Catamaran Hull Dynamic Pressure residuals at Fn=0.2453
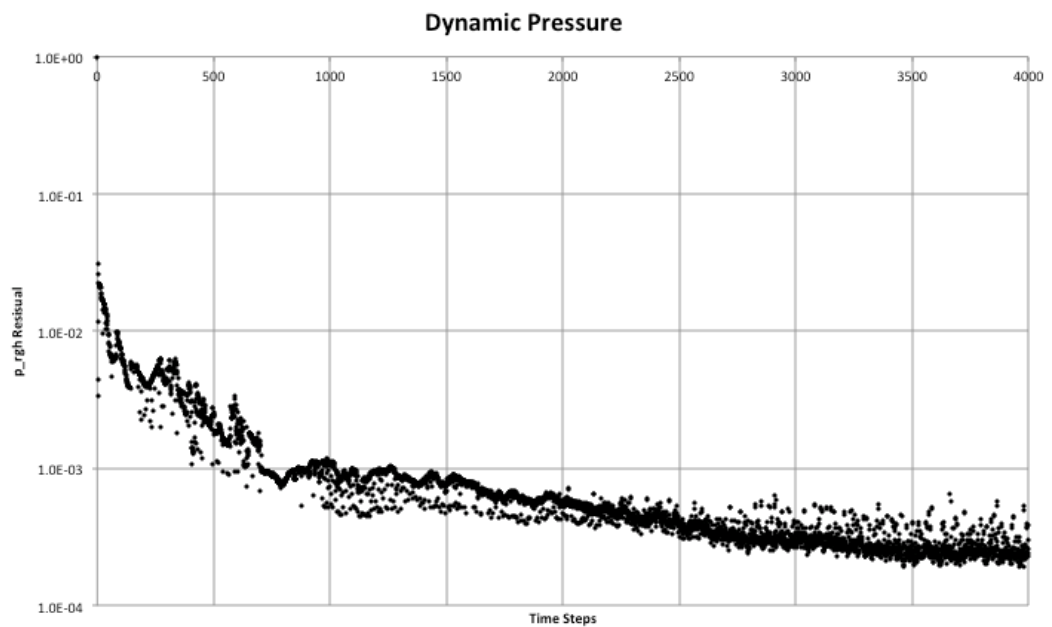
Figure 63: Catamaran Hull Dissipation rate residuals at Fn=0.2453
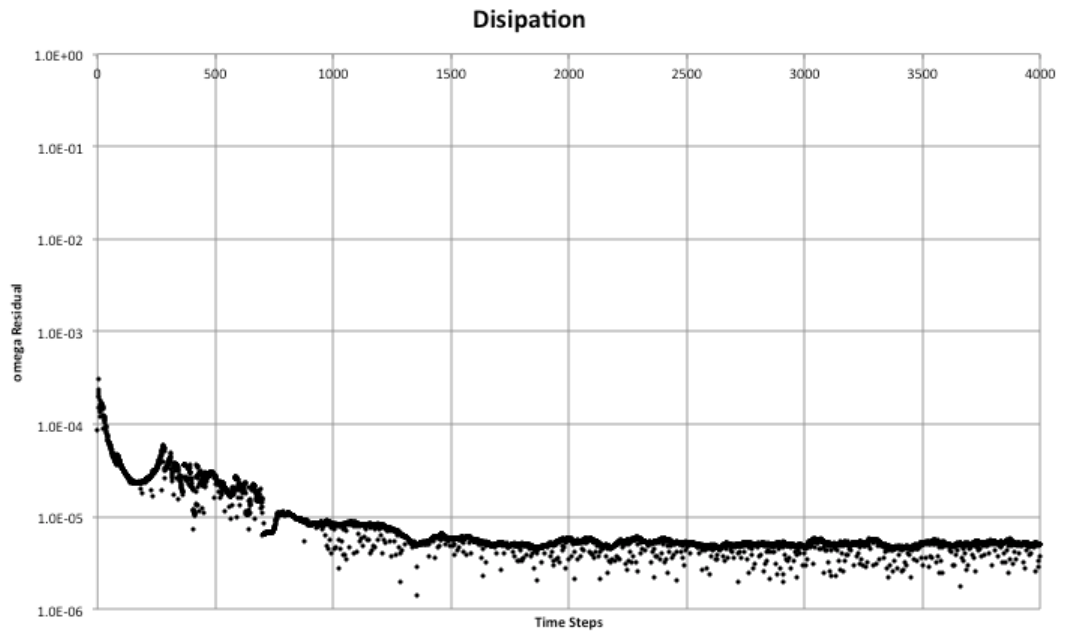
Figure 64: Catamaran Hull Turbulent Kinetic Energy residuals at Fn=0.2453
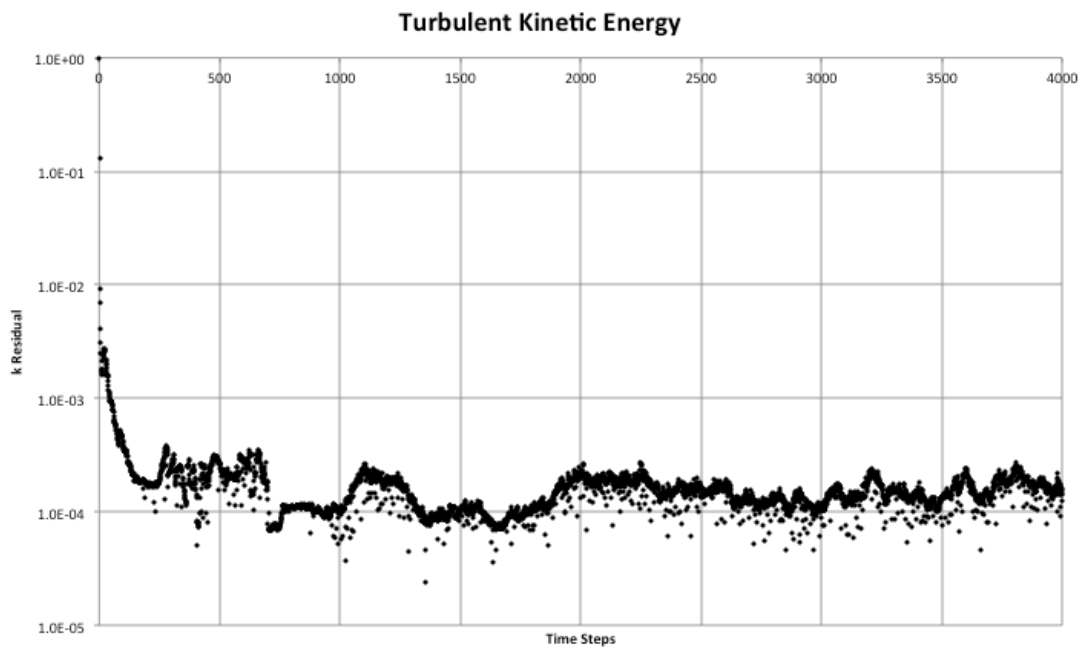
As a post-processing tool, y^+, was calculated to verify the mesh quality near the hull. A value of $y^+ \leq 100$ is acceptable for catamaran case. Figure 65 shows the wall y^+ parameter for the submerged hull.

Figure 65: y+ of water, for light condition at v=1.05 [m/s] at 4000[s]
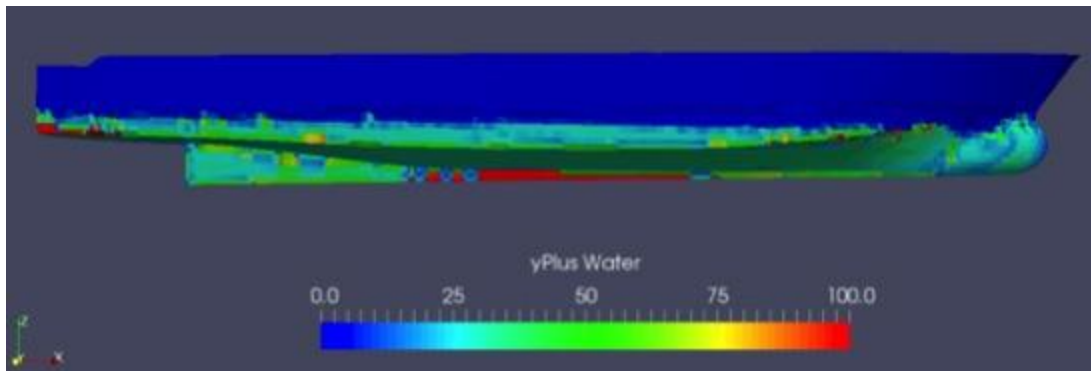
Bow, Stern and central keel are zones that required a grater mesh density.

3.4 NUMERICAL RESULTS

This section presents the numerical results from the simulation of a catamaran model of 2 [m] length using OpenFOAM. The catamaran resistance was simulated according the experimental results, using a demi and twin hull configurations. The factor of interference is also estimated.

3.4.1 Catamaran Resistance

OpenFOAM calculate the forces components acting in Catamaran hull, namely pressure and viscous. Figure 66 shows Pressure and Viscous force components for the case of demi-hull in Light Condition at a velocity of V=1.05 [m/s]. The experimental resistance is 1.79 [N] at Fn=0.2453.

Figure 66: Resistance components at V=1.05 [m/s]
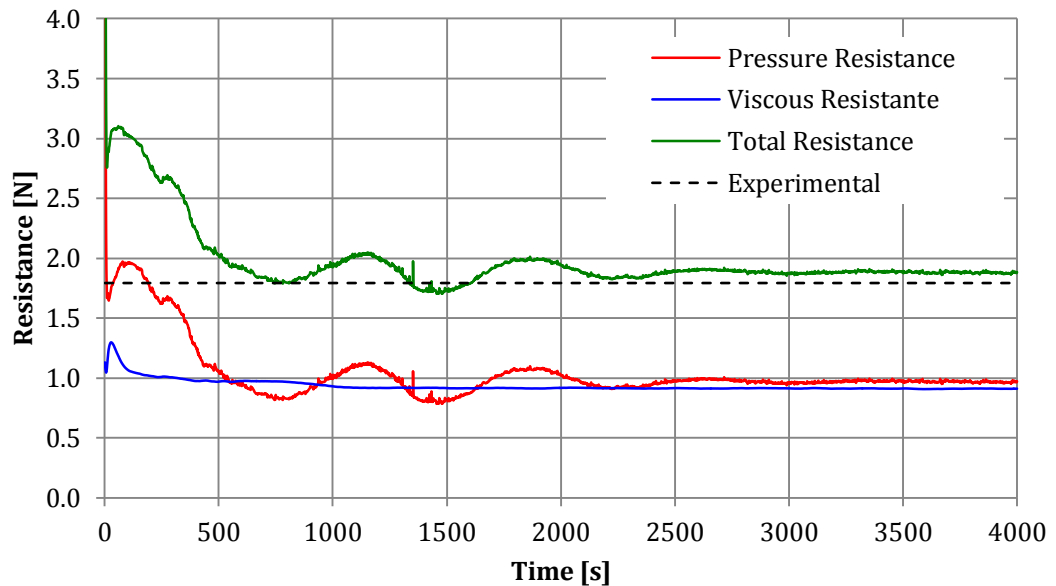
Total resistance was obtained by adding pressure and viscous forces.

3.4.1.1 Demi Hull catamaran

The model was simulated following the experimental data [1], and compared with Maxsurf-Resistance. For demi hull Maxsurf-Resistance case, Holtrop method was used, see Appendix D.

Table 22 and 23 present the data obtained by OpenFOAM simulations at different velocities in two Load Conditions. The percentage of standard deviation was obtained by [1]:

$$Sta.Dev. = \frac{Standard\ Deviation}{OpenFOAM\ average\ R_t} \tag{24}$$

Table 22: Resistance data obtained by OpenFOAM-interFOAM at different velocities – Light Load Condition – Demi hull

V[m/s]	Fn	OpenFOAM R_t [N]	Experimental R_t [N]	% Error	% Sta. Dev.
1.05	0.2453	1.88	1.79	5	0.61
1.14	0.2663	2.15	3.91	45	1.03
1.20	0.2803	1.16	3.60	68	1.71
1.30	0.3037	2.81	5.26	47	1.14
1.45	0.3387	3.54	7.01	49	1.23
			Average	42.8	1.14

Table 23: Resistance data obtained by OpenFOAM-interFOAM at different velocities – Full Load Condition – Demi hull

V[m/s]	Fn	OpenFOAM R_t [N]	Experimental R_t [N]	% Error	% Sta. Dev.
1.03	0.2393	2.08	3.08	33	0.43
1.10	0.2556	2.39	4.12	42	0.45
1.23	0.2858	2.92	4.57	36	0.64
1.35	0.3137	3.78	5.58	32	0.54
1.45	0.3369	4.43	7.00	37	0.41
			Average	36	0.50

Figures 67 and 68 shows the total resistance by OpenFOAM, experimental data and Maxsurf for demi hull.

The standard deviation of experimental data was plot. The experimental standard deviation it's about 0.63%, due this cannot be displayed. Tables 24 and 25 shows the influence of the two components of total resistance in both load conditions for demi and twin hull, respectively.

Figure 67: Total resistance of demi catamaran hull at different Froude number – Ligth Condition
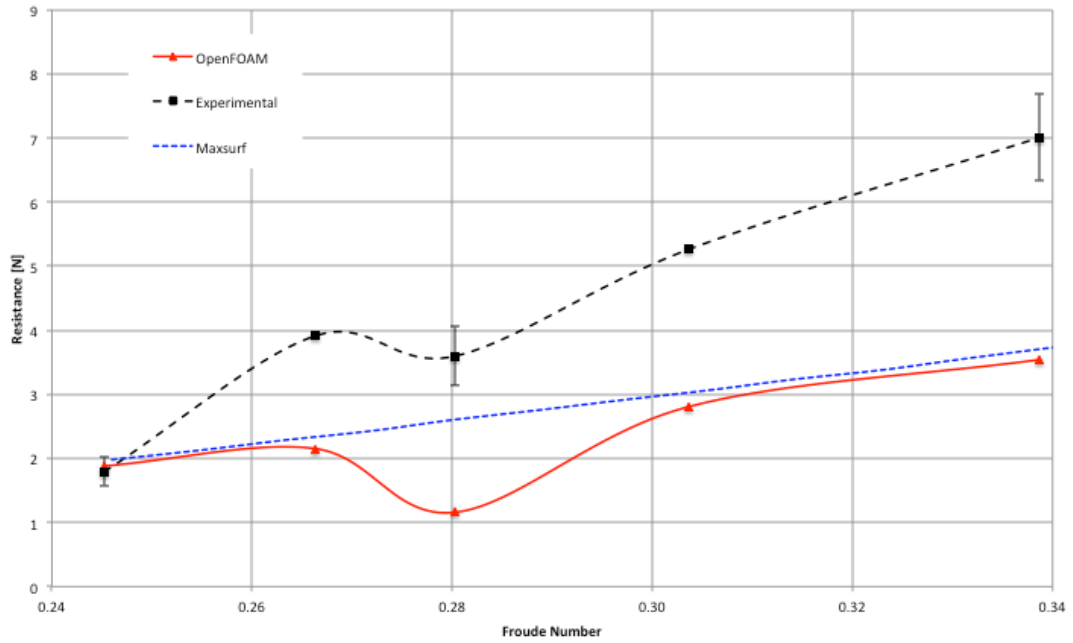
Figure 68: Total resistance of demi catamaran hull at different Froude number – Full Condition
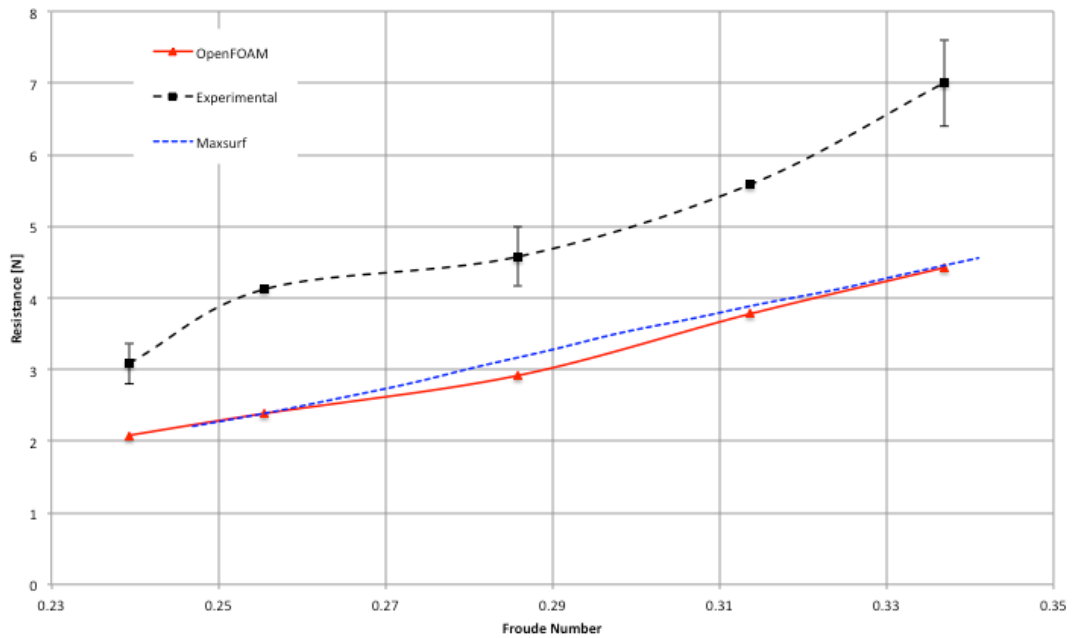
Table 24: Total resistance components for Demi hull

Demi Hull					
Light Condition			Load Condition		
Fn	Resistance due to Pressure	Resistance due to Viscosity	Fn	Resistance due to Pressure	Resistance due to Viscosity
0.2453	0.97	0.91	0.2393	1.05	1.03
0.2663	1.06	1.09	0.2556	1.21	1.18
0.2803	1.13	0.03	0.2858	1.47	1.44
0.3037	1.42	1.39	0.3137	2.05	1.73
0.3387	1.78	1.76	0.3369	2.46	1.97

Table 25: Total resistance components for Twin hull

Twin Hull					
Light Condition			Load Condition		
Fn	Resistance due to Pressure	Resistance due to Viscosity	Fn	Resistance due to Pressure	Resistance due to Viscosity
0.2453	1.96	1.91	0.2440	2.21	2.15
0.2663	2.10	2.22	0.2602	2.47	2.40
0.2943	2.69	2.67	0.2904	3.19	2.95
0.3083	3.16	2.93	0.3090	4.21	3.31
0.3434	3.87	3.59	0.3392	5.74	3.90
0.3574	4.15	3.86	0.3602	5.81	4.39
0.4111	7.03	4.94	0.4066	8.66	5.58
0.4532	9.47	5.93	-	-	-

3.4.1.2 Twin Hull catamaran

The model was simulated following the experimental data [1], and compared with Maxsurf-Resistance. To simulate the catamaran structure in OpenFOAM, the hull was displaced into the computational domain a distance S=0.2805 [m], measured from the centerline of ship to centerline of the hull, Figure 69

shows the distribution. For demi hull Maxsurf-Resistance case Molland method was used, see Appendix D.

Figure 69: Twin catamaran domain geometry with a separation of S=0.2805 [m]
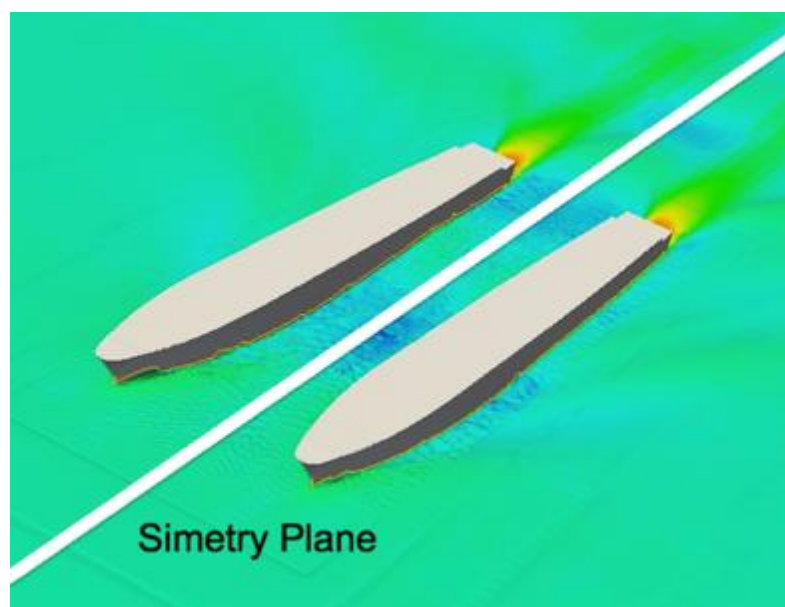
Table 26 and 27 present the data obtained by OpenFOAM simulations at different velocities in two Load Conditions.

Table 26: Resistance data obtained by OpenFOAM-interFOAM at different velocities – Light Load Condition – Twin hull

V [m/s]	Fn	OpenFOAM	Experimental	% Error	% Sta. Dev.
1.05	0.2453	3.87	5.11	24	0.60
1.14	0.2663	4.51	4.80	6	0.51
1.26	0.2943	5.36	6.14	13	0.50
1.32	0.3083	6.08	7.76	22	0.75
1.47	0.3434	7.45	8.09	8	0.51
1.53	0.3574	8.01	10.32	22	0.51
1.76	0.4111	11.97	12.07	1	0.38
1.94	0.4532	15.40	13.29	16	0.48
			Average	14	0.53

Table 27: Resistance data obtained by OpenFOAM-interFOAM at different velocities – Full Load Condition – Twin hulls

V [m/s]	Fn	OpenFOAM	Experimental	% Error	% Sta. Dev.
1.05	0.2440	4.36	7.91	45	0.51
1.12	0.2602	4.87	6.88	29	0.61
1.25	0.2904	6.13	10.06	39	0.64
1.33	0.3090	7.52	10.54	29	0.45
1.46	0.3392	9.64	12.14	21	0.35
1.55	0.3602	10.20	14.54	30	0.46
1.75	0.4066	14.24	20.62	31	0.33
			Average	32	0.48

Figures 70 and 71 shows the total resistance by OpenFOAM, experimental data and Maxsurf for demi hull.

Figure 70: Total resistance of catamaran hull at different Froude number – Ligth Condition
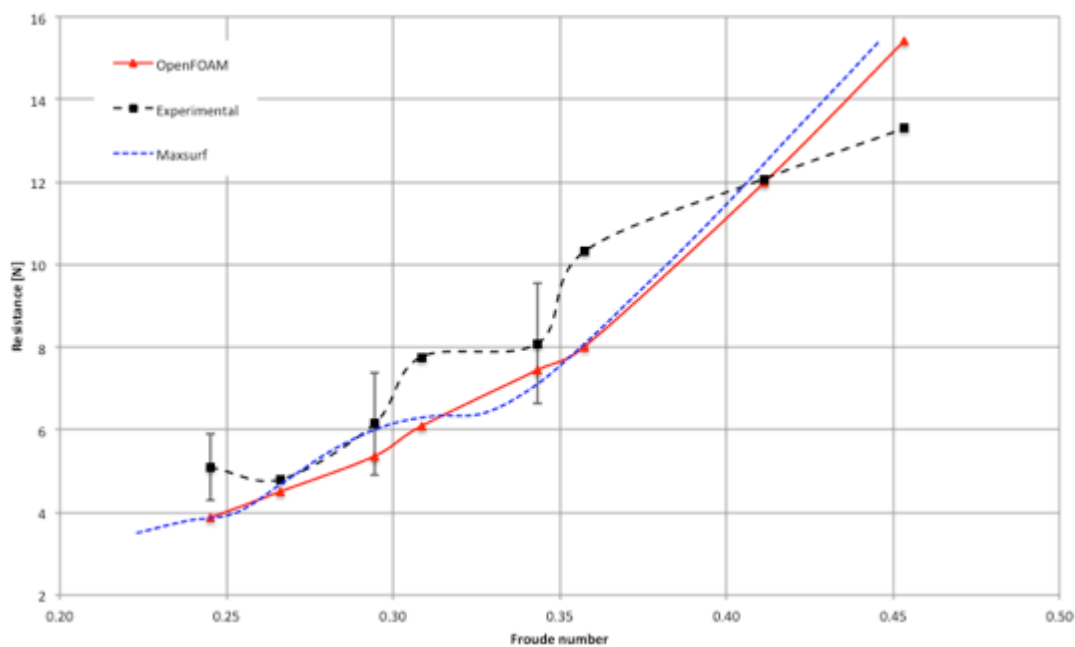
Figure 71: Total resistance of catamaran hull at different Froude number – Full Condition
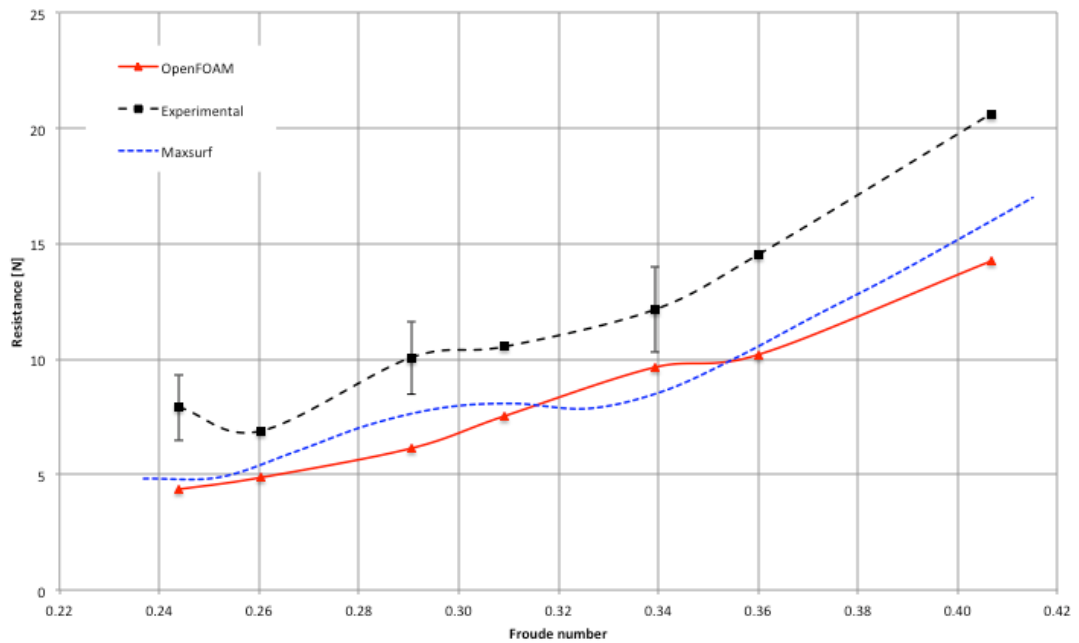
The errors between experimental data and numerical simulations are lower in light condition of catamaran. However none of the curves follows the same trend.

3.4.1.3 Numerical estimation and prototype comparison

Figure 72 shows the data obtained by sea test. This data was not directly compared with the numerical resistance because was tested in other load condition. However, for Froude numbers greater than 0.30 the resistance is between the light and full load condition, which was expected because the real data was tested in a intermediate load condition.

Figure 72: Catamaran total resistance at a medium load condition, draft=0.0948 [m]
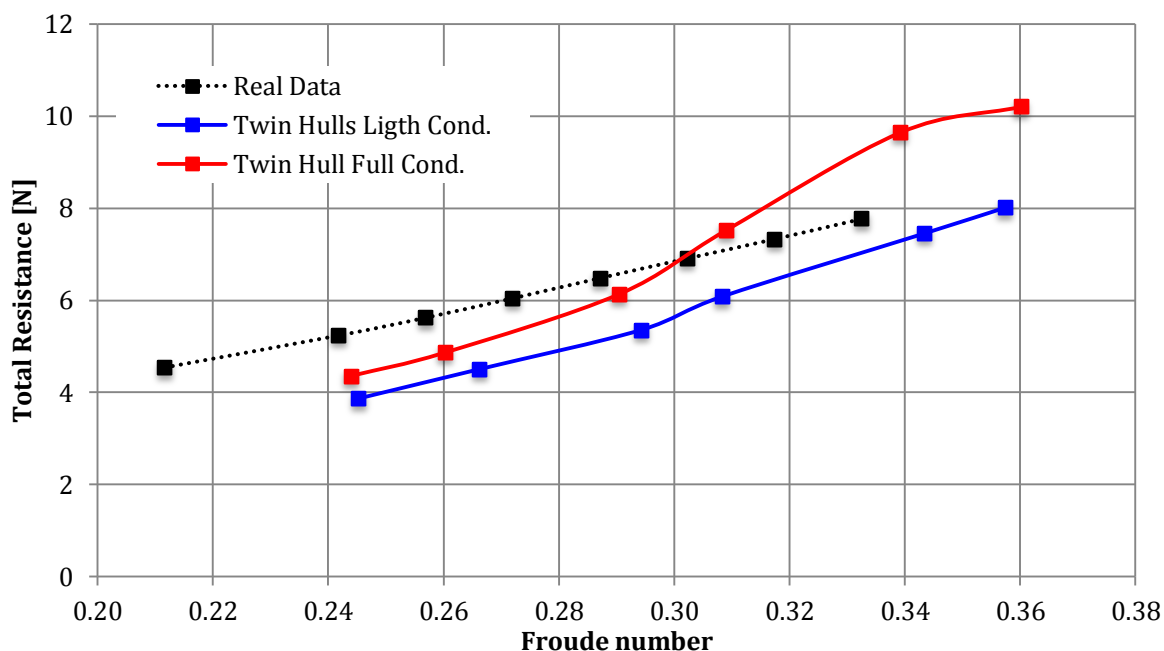
3.4.1.4 Pressure Distribution

Figures 73 to 75 shows the pressure distribution the hull for Fn=0.34 (v=1.45 m/s). The labels of dynamic pressure was setting to capture as blue ones the zones with negative pressure and red ones the zones with positive pressure. The 3 zones (stern, middle section and bulbous), where there is a wave crest, the pressure increases. In the case of the twin hulls, the pressure in the inner side of the hull is slightly greater than the pressure on the outside of the hull; this is due to the interference caused by the other hull.

Figure 73: Outside Demi hull dynamic pressure around the hull at Fn=0.34 Full Load
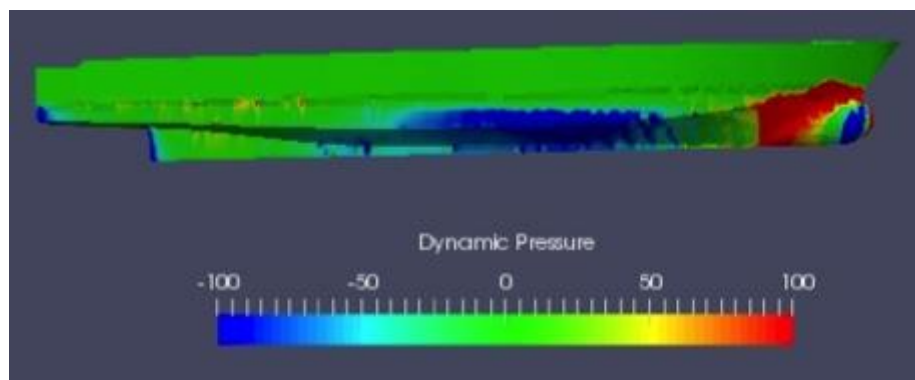
Figure 74: INSIDE Twin hull dynamic pressure around the hull at Fn=0.34 Full Load
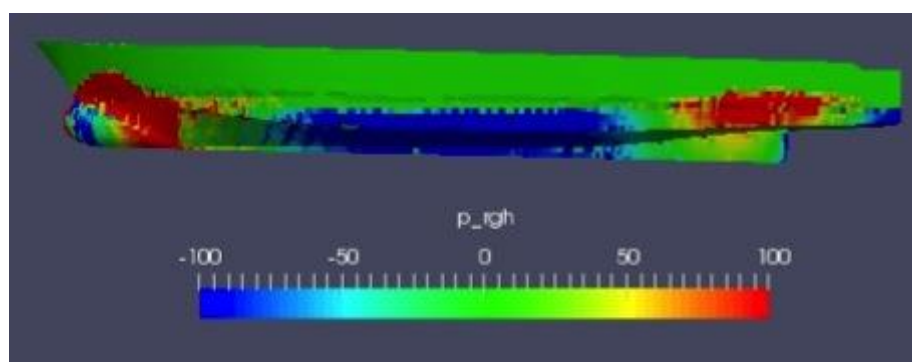
Figure 75: OUTSIDE Twin hull dynamic pressure around the hull at Fn=0.34 Full Load
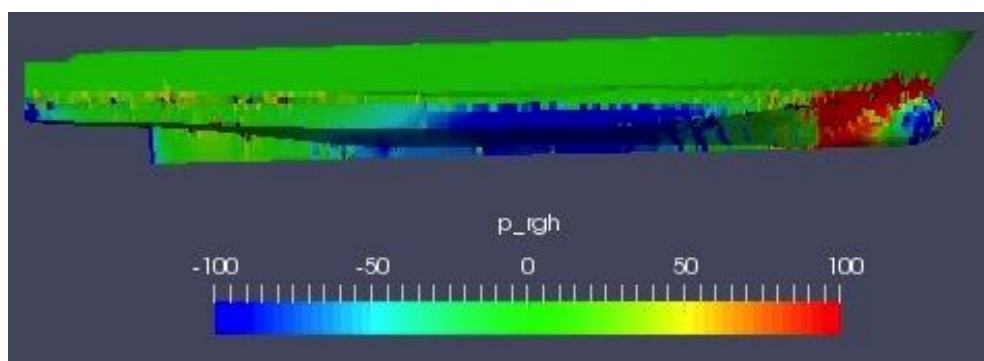
Bolbuos is the zone with greater pressure; Figure 76 shows the pressure in this zone, outside the hull.

Figure 76: Pressure around the bulbous for Twin hull at Fn=0.34 Full Load, right-inside the two hulls
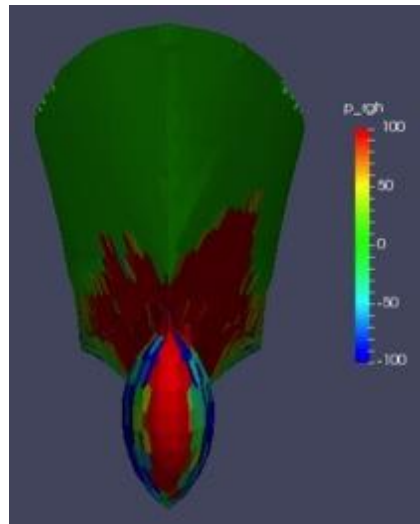
3.4.2 Interference factor between hulls

The catamaran interference was estimated following the expression [1]:

$$R_W = \frac{R_{T\ CAT} - 2\ R_T}{2} \tag{25}$$

Where:

R_W is the demi hull interference in Newton

$R_{T\ CAT}$ is the total resistance of twin hulls in Newton

R_T is the ttal resistance of demi hull in Newton

Figure 77 and 78 shows the interference factor for original hull separation at Light and Full load conditions.

Figure 77: Interference for Light load condition
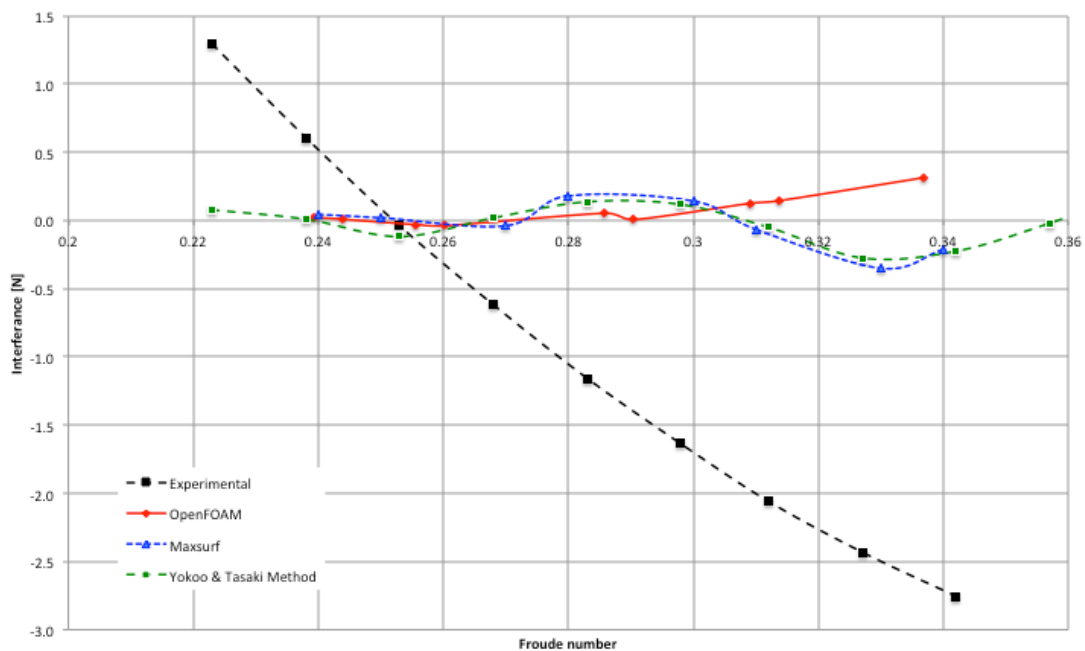
Figure 78: Interference for Full load condition
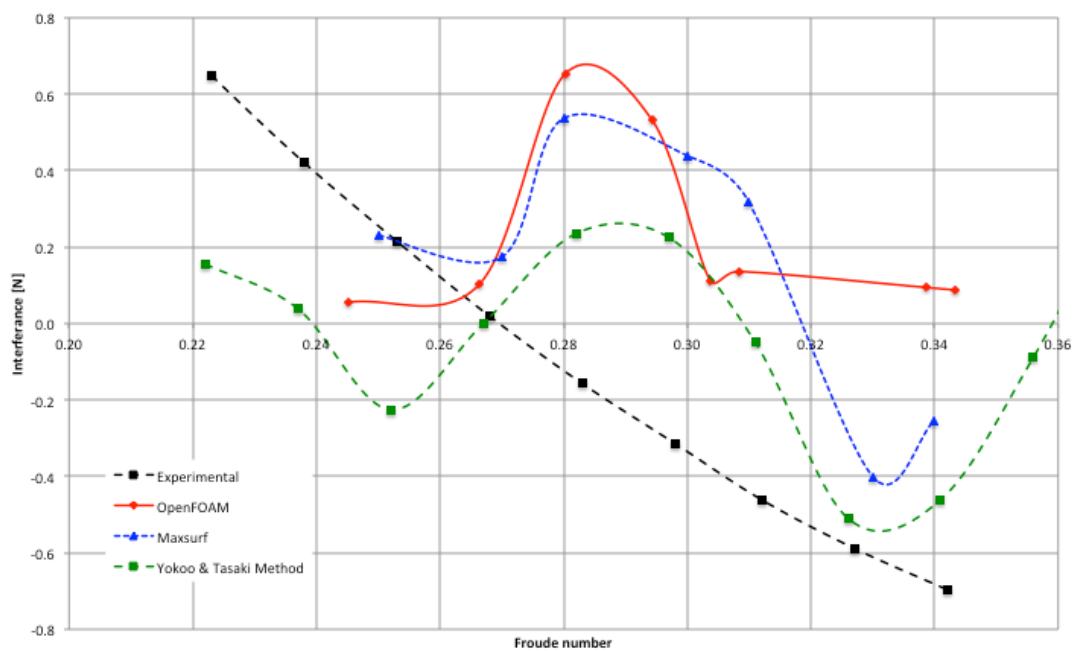
The interference factor obtained by numerical simulations is linear contrasting with the experimental interference published by Chávez and Lucín [1]. The positive interference corresponds to increased interference (unfavorable) and the negative values to decrease (favorable).

3.4.3 Wave pattern

Figure 79 to 81 shows the wave pattern for different Froude numbers in Full load condition.

Figure 79: Wave pattern at Fn=0.24
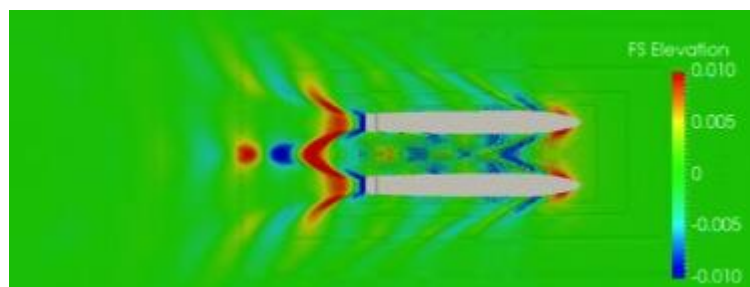
Figure 80: Wave pattern at Fn=0.31
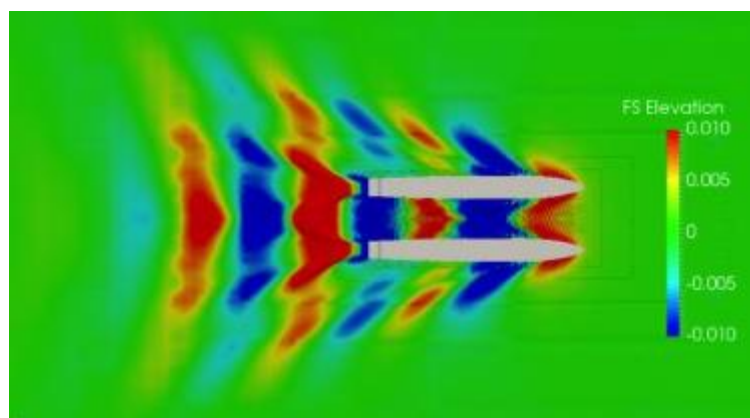
Figure 81: Wave pattern at Fn=0.34
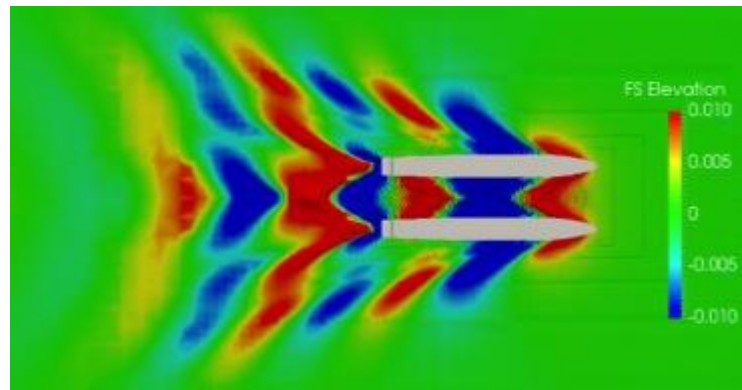
The blue areas correspond to the hollow of the wave and the red areas to the hump.

CONCLUSIONS

Before starting the Catamaran numerical resistance, several tutorials were performed using the OpenFOAM user manual [1]. These tutorials were of great help to understand the capabilities and limitations of the software. *Cavity* was the first made tutorial, for laminar and incompressible flows. The user manual gives an overview of the workflow of OpenFOAM: Pre-processing, solution and Post-processing. ParaView is a post-processing tool; the user manual also gives an introduction of its operation. This was an important step for understanding OpenFOAM and the principles of fluid analysis.

Then, DTC Hull tutorial was performed. All the tutorial chapters were reviewed to understand the simulation procedure. The first simulation performed was with the original settings, with 8 processors working in parallel. Later, others simulations were performed using different numbers of processors to understand how the domain could be decomposed. The lowest time of resolution was with 12 processors, but the difference between 8 and 12 processors was of 10 minutes. For this reason, and to save computational resources, the following simulations were performed with 8 processors.

A mesh convergence study was developed for DTC Hull. Starting from the tutorial mesh, three meshes were created: 2 with lower density and one with more density than the tutorial. Unfortunately, the mesh with the highest

density exploded due the instabilities associated with turbulence models, and it was not considered in the present study. The tutorial mesh had the lowest error against the experimental data, 0.25% at Fn=0.218.

Two solvers were used in DTC hull study, interFOAM and interDyMFOAM. The two methods differ mainly in the procedure of meshing; interDyMFOAM has a dynamic mesh motion and gives 2 degrees of freedom to the hull. The average errors between interFOAM and interDyMFOAM versus experimental data were of 5.42% and 3.79%, respectively. The resistance of interDyMFOAM solver seems more reliable and the trend of the resistance curve is very similar to the experimental data. Nevertheless, the time of resolution is too long compared to interFOAM solver, there are a difference of 18 hours (interFOAMTimeSolution=2.74 h, interDyMFOAMTime Solution=20.97 h).

The same process as DTC hull was followed for the Catamaran. A catamaran mesh convergence study was develop first, with 3 types of mesh for a demi hull at Fn=0.2453. Mesh 2, with 1 million of cells, was chosen to the simulation because had the lowest error and standard deviation at R_{texp}=1.79 [N], error=5% and Sta. Dev.=0.34 [N]. Due the extensive time of resolution, interDyMFOAM solver was not considered in Catamaran hull. Two load conditions were implemented for demi and twin hulls. The errors for Light

Load Condition were: 42.8% in Demi Hull and 14.0% in Twin Hull configurations. The errors for Full Load Condition were: 36.0% in Demi Hull and 32.0% in Twin Hull configurations.

Numerical simulations using OpenFOAM are a feasible method for predicting the resistance of Cormorant Evolution catamaran, despite the difference between experimental data and numerical simulation resistance. However, numerical results are close to statistical methods, as Holtrop and Molland, estimated with Maxsurf Resistance software.

The interference component between the twin hulls was estimated for Full and light Load conditions for Fn between 0.24 and 0.34. But these results were not that expected, because the curves of interference didn't have the same trend. Also, the interference factor was calculated using the Maxsurf data and even though was not very close, Maxsurf interference had the same trend against numerical data.

These variations between experimental results and numerical simulations may be due to external factors, that can not be controlled or measured, such as: wind, water temperature, interference between the method of drag, towing velocity uncertainly, differences between the model and the catamaran, and range of work of Data Card available in our college.

RECOMMENDATIONS

Understand the turbulence modeling used in DTC Hull and the others turbulence models available in OpenFOAM, is a good start to improve the numerical simulations.

The meshing process is one of the most conflictive steps in the numerical simulation. Find the mesh density according the areas of the ship, bow or aft, is important to the VoF in the following steps.

Assessing the data generated by OpenFOAM numerical simulations, experiments and Maxsurf Resistance software. It seems possible to suggest the redesign of the current system implemented in the experimental tests on ESPOL Lake to reduce its experimental uncertainty or buying a data card with a lower range of work, because the standard deviations were around 20% and less than 1% in the numerical simulations.

FUTURE WORK

For the continuation of this work, the implementation of InterDyMFOAM solver is recommended. This method was not used Catamaran resistance due to limited time and the need of more computational resources.

The Catamaran Cormorant Evolution provides tourist services in the Galapagos Islands. Due this, a study of resistance in shallow water is recommended, following the regulations given by Ecuador for this protected area. This study can be developed by theoretical, experimental and numerical method for its comparison.

Due to the error between experimental data and numerical simulations, a redesign of the experimental test and new test resistance for Catamaran Cormorant Evolution is recommended for future work.

For DTC Hull, understand why the simulation with more number of elements did not work. This is important because with more number of elements the geometry of hull will be more real.

BIBLIOGRAPHY

[1] **Lucín A. & Chávez J.** "Estudio experimental de la influencia de la separación de los cascos sobre la Resistencia en un catamarán de 32.5 metros", 2012.

[2] **Holtrop J. & Mennen G.G.J.** "An approximate power prediction Method", 1984

[3] **Yokoo K. & Tasaki Ryo**, Technical Report No1: "On the twin hull ship" of the University of Michigan, 1951.

[4] **The Society of Naval Architects and Marine Engineers-SNAME,** Principles of Naval Architecture, December 1966.

[5] **ESI**, OpenFOAM, www.openfoam.com

[6] **Bertram V.,** Practical ship hydro dynamics, 2000.

[7] **Astillero y Marina BOTTO CIA. LTDA.**, Memoria Técnica del Catamarán "Cormotant Evolution", 2010.

[8] **OpenFoam,** The Open Source CFD Toolbox User Guide, Version 3.0.1, 13th December 2015.

[9] **Ould el Moctar, Vladimir Shigunov & Tobias Zorn**, Duisburg Test Case Port-Panamax Container Ship for Benchmarking, Ship Technology Research Schiffstechnik VOL.59 / No.3, August 2012.

[10]   **J. P. Laval.** Unsteady Simulations on Turbulence Flows (DNS & LES), Laboratoire de Mécanique de Lille (LML), CNRS. France 2006.

[11]   **David C. Wolcox,** Turbulence Modeling for CFD, DCW Industries, Third Edition, November 2006.

[12]   **Petros Voxakis,** Ship Hull Resistance Calculations Using CFD Methos, Naval Engineer and Master of Science in Mechanical Engineering at the Massachusetts Institute of Technology. May 2012.

[13]   **Menter, F.R., Kuntz, M. and Langtry, R.** Ten Years of industrial experience with the SST turbulence model. Turbulence, Head and Mass Transfer 4. Edited by K. Hanjalic, Y. Nagano, and M. Tummers. New York. 2003.

[14]   **Bondi, André B.** Characteristics of scalability and their impact on performance. Proceedings of the second international workshop on Software and performance – WOSP. 2000.

[15]   **Nelson, B**. (2013). The 6DF IMU 6-D motion variant provides six dimensional motion sensing over six degrees of freedom by sensing translation movement in three perpendicular axes (surge, heave, sway) nd rotational movement in three perpendicular axes (roll, pitch, yaw), 2013.

[16]   **Boat Design forum,** "Mass and moment of inertia forum", www.boatdesign.net, USA 2004.

[17]   **Rhinoceros,** Rhinoceros 5 - 90 days trial, https://www.rhino3d.com/es.

[18]   **Benites D.** "Pruebas experimentales para determiner la influencia de Flaps en la resistencia al avance de una lancha planeadora de 11 metros". 2012

[19]   **Maxsurf,** Maxsurf Modeller, http://www.maxsurf.net

[20]   **openSUSE,** Basic commands, http://www.opensuse.org

[21]   **ParaView**,   ParaView   4.4.0   tutorials, http://www.paraview.org/tutorials/

[22]   **Menter, F.R., Kuntz, M. and Langtry, R.** Ten Years of industrial experience with the SST turbulence model. Turbulence, Head and Mass Transfer 4. Edited by K. Hanjalic, Y. Nagano, and M. Tummers. New York. 2003.

APPENDICES

Appendix A: openSUSE Basic Command Cheat Sheet

openSUSE Basic Command Cheat Sheet

Accounts

To create a new user account

```
# useradd <name>
        -u specific UID
        -g specific GID
        -d create home dir
        -c User full name
        -s Assign a Default Shell
```

Example

```
# useradd jsmith -u 1010 -g
501 -d /home/users/jsmith -c
"Joe Smith" -s /bin/bash
```

To add/change a password

```
# passwd <name>
```

To Modify a user account

```
# usermod <name>

        -c Changes the user name
# usermod -c "Joe Smith" jsmith
        -G add a user to a group
# usermod -G homeuser jsmith
        -L Lock the user account
# usermod -L jsmith
        -U Unlock the user account
# usermod -U jsmith
        -s Change or set a shell
# usermod -s /bin/tcsh jsmith
```

Change a User Shell

```
# chsh -s /bin/<shell> <name>
```

Deleting User Accounts

```
# userdel <name>
```

RPM

Installing an RPM

```
# rpm -ivh <package>
```

Upgrading an RPM

```
# rpm -Uvh <package>
```

Removing an RPM *

```
# rpm -e <package>
```

Detials about an install RPM

```
# rpm -qi <package>
```

List the contents of an RPM

```
# rpm -qlp <package>.rpm
```

List installed RPM'es

```
# rpm -qal
```

Example to find an installed RPM

```
# rpm -qal | grep <package>
```

To see what provides a command

```
# rpm -q –whatprovides <name>
```

YaST

Run YaST in QT Graphical Frontend

```
# yast --qt
```

Run YaST in gtk Graphical Frontend

```
# yast --gtk
```

Run YaST in text-mode frontend

```
# yast --ncurses
```

Install a Package with YaST

```
# yast -i <package>.rpm
```

Remove an Installed Package with YaST

```
# yast --remove <package>.rpm
```

List all available Module

```
# yast -l -or- yast --list
```

To obtain usage of a module

```
# yast <module> help
```

* Do recommend using the rpm -e. It can break other packages

Using the Shell

To see what current shell is set	To see who you are	Change directory
# echo $SHELL	# whoami	# cd <directory>
Display all of the settings	**To see history**	**Go back the last directory**
# set	less	# history	# cd -
List Bash Settings	**Log in as Superuser**	**To repeat the last command**
# env	# su -l	# !!
To find a command you have ran	**Watch a file**	**To see the current time**
# ctrl-r <start typing the command>	# tail -f <file>	# date

openSUSE Basic Command Cheat Sheet

SaX

Set Graphics Card
```
# SaX2
```

Using SaX to Config ATI Card
```
# SaX2 -r -m 0=radeon

# SaX2 -r -m 0=fglrx
```

Using SaX to Config Nvidia
```
# SaX2 -r -m 0=nv

# SaX2 -r -m 0=nvidia
```

Services*

List all Services
```
# service –status-all
```

To get a status on a Service
```
# service <name> status
```

To start a Service
```
# service <name> start
```

To stop a Service
```
# service <name> stop
```

To restart a Service
```
# service <name> restart
```

To do a full-restart on a Service
```
# service <name> --full-restart
# service -full-start <name>
```

To do a reload
```
# service <name> reload
```

File Systems

To list all disk and partitions
```
# fdisk -l
```

To list for a specific disk
```
# fdisk -l /dev/<h/s>d<a-z>
```

List mounted file systems
```
# mount
# cat /proc/mounts
```

List only specifics system type
```
# mount -t <type>
```

List all mounted ext3 system type
```
# mount -t ext3
```

Mount partition
```
# mount -t <type> <device> <mount point>
```

Example Mount
```
# mount -t ext3 /dev/sda1 /mnt
```

Mount CD/DVD ISO as a loopback Device
```
# mount -t iso9960 -o loop name.iso <mount>
```

Example of mounting a saved iso as a loopback device
```
# mount -t iso9960 -o loop /tmp/opensuse-11.2-x86_64.iso /mnt
```

See status of loopback devices
```
# losetup -a
```

Unmount File Systems
```
# umount /dev/<device>
# umount /<mount point>
```

Process

Show Every Process Currently Running

```
Every running Process
# ps -e

Every running Process, long listing
# ps -el

Every running Process, full-format listing
# ps -ef

Every running Process, Short BDS Style
# ps ax

Every running Process, Long BDS Style
# ps aux
```

Show Memory Use
```
# free -o -m
```

Current open files and directories
```
# lsof | less
```

View Ethernet Connection
```
# ifconfig -a
```

View Wireless Interface
```
# iwconfig
```

**Show Routes**
```
# route
# netstat -rn
```

Show all open ports
```
# netstat -anp
```

* With openSUSE you can find most services under */usr/sbin* with *rc* in front. So you can the replace service with **rc<name> <action>**, example **# /usr/sbin/rcapache2 restart**

Appendix B: VNC remote –ssh connection

1. Open the terminal from Launchpad (OS X-Macbook Pro)

2. In the terminal write: *ssh –L5902: localhost:5902*

   username@IPnumber

3. Write the password: *******

4. Wait until your connect

5. Open VCNViewer program from the Launchpad
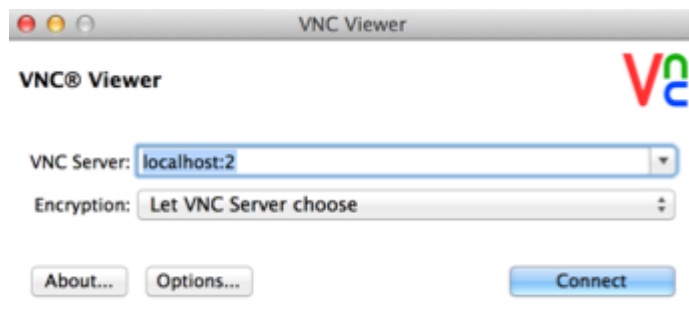
6. VNC Server: *localhost:2*

7. VNC password: ******

8. Finally, a virtual window will show you the environment of WorkStation

Appendix C: ParaView remote –ssh connection

1. Open the terminal from Launchpad (OS X-Macbook Pro)

2. In the terminal write: *ssh –L5558:localhost:5558 username@IPnumber*

3. Write the password: *******

4. Disable virtual window to open ParaView, write on the terminal:

   pvserver --server-port=5558 --use-offscreen-rendering --multi-clients

5. ParaView have to be installed at the computer or laptop. Open ParaView from the Launchpad and chose Server Configuration – Add Server
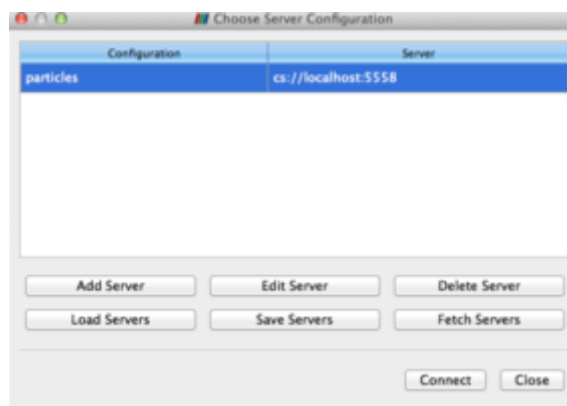


6. The new server configuration is:
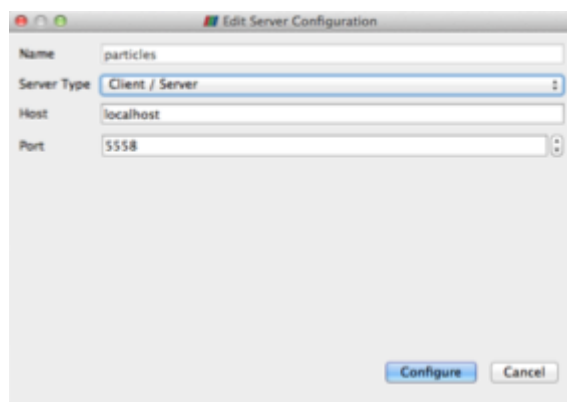
7. Press Configure

8. In the ParaView toolbar, Main controls chose Connect

9. In the ParaView toolbar go to *File – Open* and chose the file to open:

    FileName.OpenFOAM

Appendix D: Maxsurf – Resistance

Catamaran geometry developed in Rhinoceros 5 was exported as a (.iges) format. Initial Graphics Exchange Specification (.iges) is one of the formats that support Maxsurf. At first, the Catamaran geometry was imported to Maxsurf modeler. This module of Maxsurf avoids the design, modeling and modification of ships geometries. Here, demi and twin hulls were setting in a specific frame of reference and zero point and save it as a (.msd) file. Figure 82 shows the workspace.

Figure 82: Maxsurf modeler workspace – Catamaran geometry
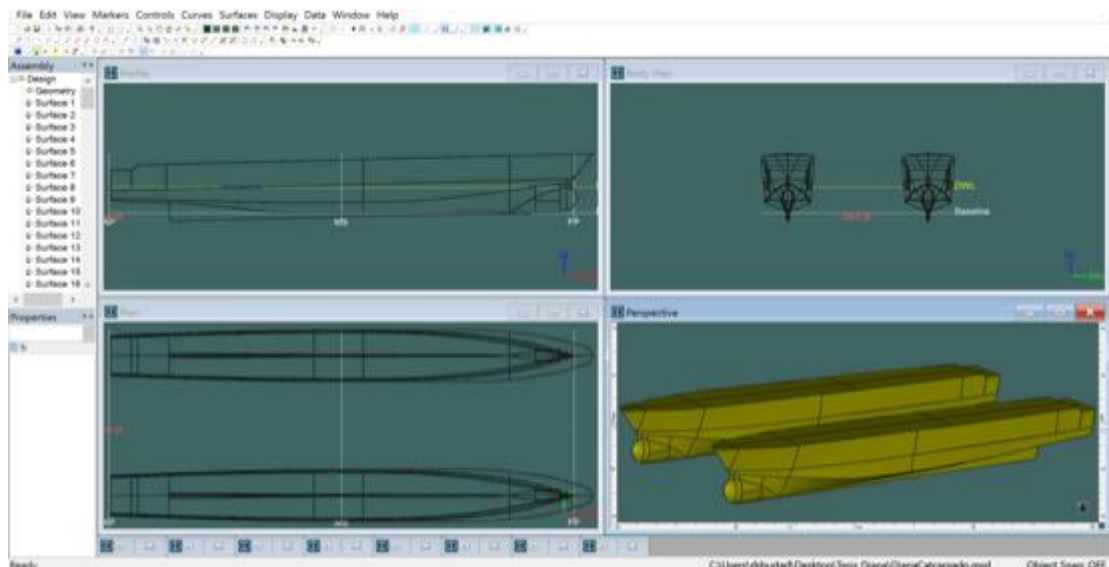
Maxsurf Resistance module it's a wave and power prediction tool. Use a range of industry standard algorithms, allowing the user to select the method to implement. The calculations methods that provided Maxsurf for resistance are: Savitsky pre-planning and planning; Lahtiharju for planning vessels;

Blount & Fox for planning vessels, Holtrop and Compton for fast displacement hulls; Fung and Series 60 for ships; van Oortmerssen for full form hulls such as tugs and trawlers; and Delft systematic yacht series for sailing yachts. It is also possible to directly analyze the resistance of a MAXSURF hull using a Slender Body method, which uses a potential flow CFD approach. For catamaran, Holtrop and Molland methods were implemented.
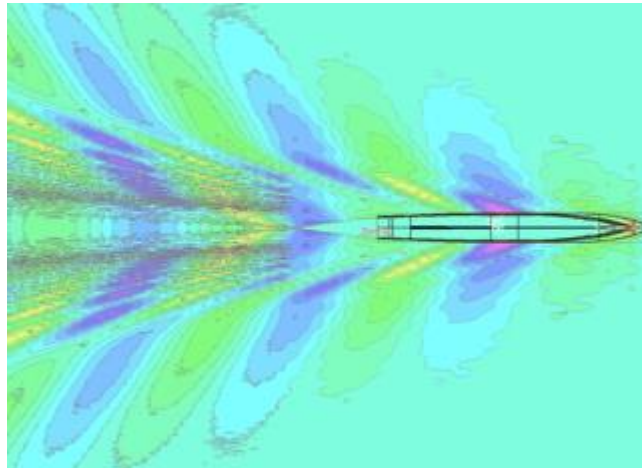
Figure 83: Maxsurf Resistance workspace
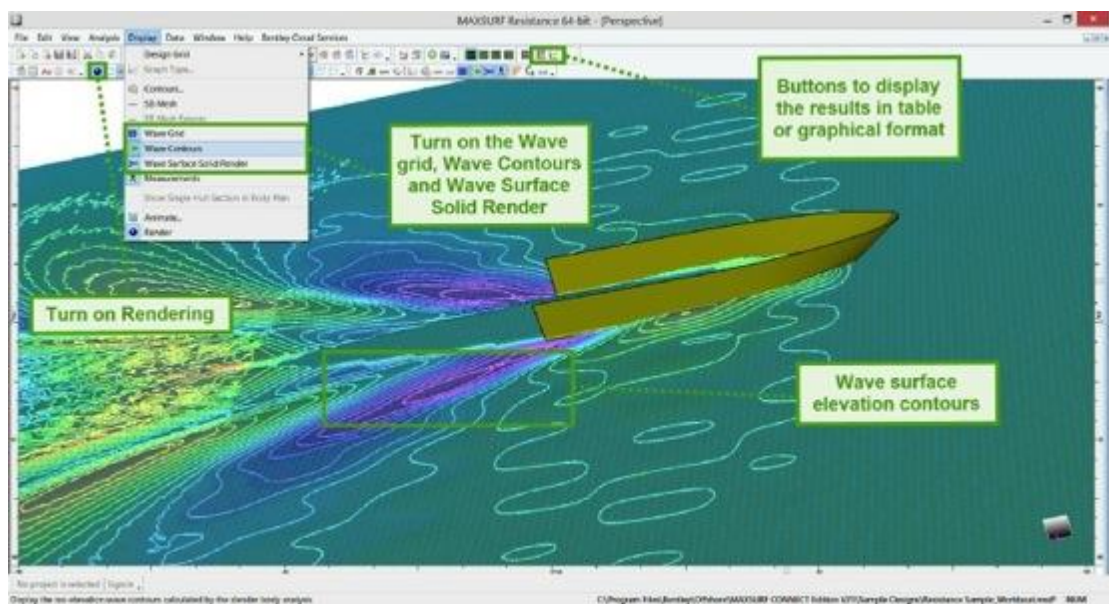
Following, Figures 84 to 87 shows the wave surface elevation contours for demi and twin hulls at Fn=0.34 in two Load Conditions.

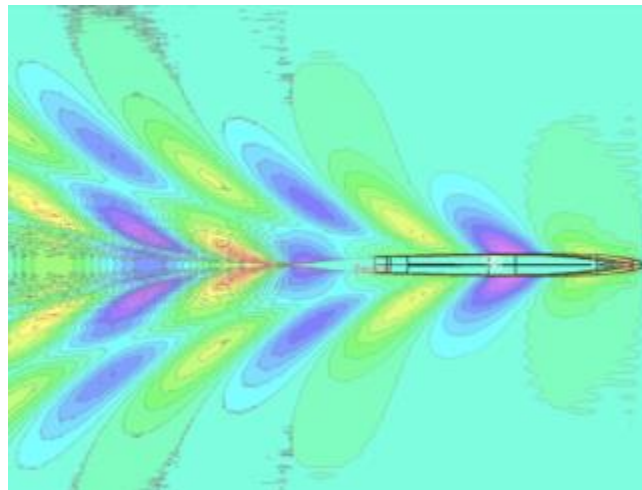**Figure 84:** Maxsurf wave height for a demi hull at Light condition and
Fn=0.34

Maximum wave height=0.1251 [m]
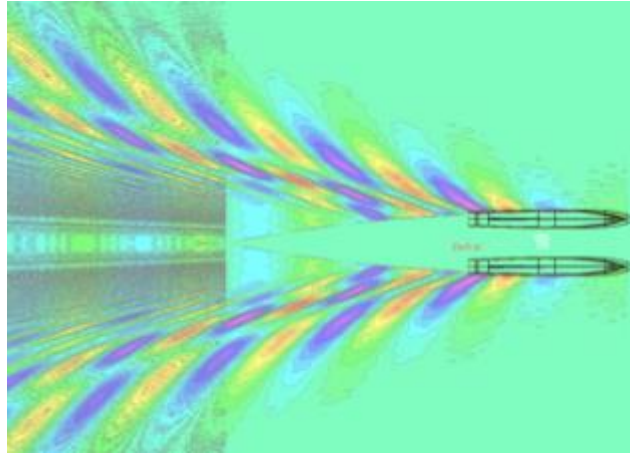
Minimum wave height=-0.0787 [m]

Figure 85: Maxsurf wave height for a demi hull at Full condition and Fn=0.34

Maximum wave height=0.1252 [m]

Minimum wave height=-0.0821 [m]
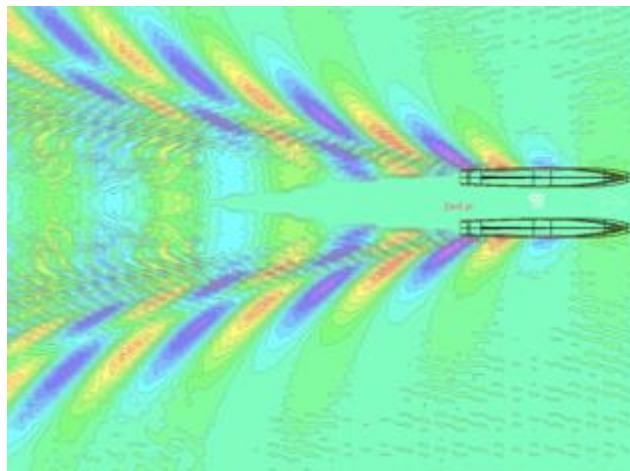
Figure 86: Maxsurf wave height for a twin hull at Light condition and Fn=0.34

Maximum wave height=0.2503 [m]

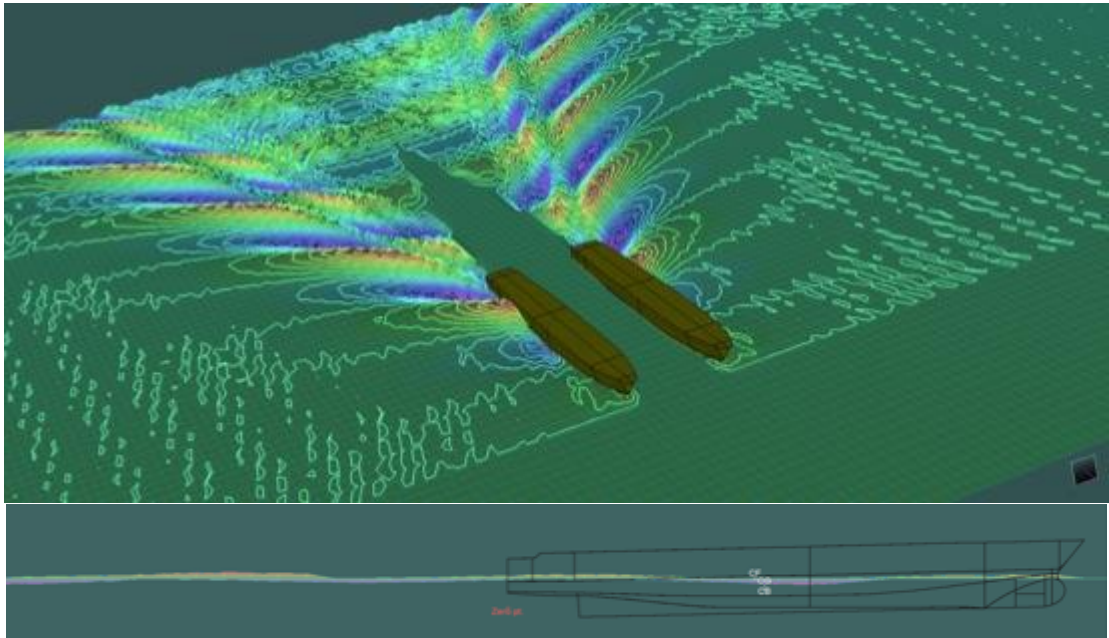Minimum wave height=-0.0803 [m]

Figure 87: Maxsurf wave height for a twin hull at Full condition and Fn=0.34

Maximum wave height=0.2724 [m]

Minimum wave height=0.0844 [m]

Figure 88: Perspective view - Maxsurf resistance for a twin hull at Load condition and Fn=0.34

Holtrop & Mennen Method

The method of Holtrop and Mennen is used to estimate the resistance of displacement ships. It is based on a statistical regression of model test and results from ship trials. Holtrop and Mennen database covers a wide range of ship [2].

Table 28: Range of application of Holtrop and Mennen method

Type of Ship	F_n max	C_p		L_{wl}/B_{wl}		B_{wl}/T_m	
		min	max	min	max	min	max
Bulkcarriers	0.24	0.73	0.85	5.1	7.1	2.4	3.2
Tugboats	0.38	0.55	0.65	3.9	6.3	2.1	3.0
Containership	0.45	0.55	0.67	6.0	9.5	3.0	4.0
General Load	0.30	0.56	0.75	5.3	8.0	2.4	4.0
Roll-on Roll-off and Ferries	0.35	0.55	0.67	5.3	8.0	3.2	4.0

Catamaran Demi Hull was considerate as a General Load Ship with the following values:

Fn=0.28

Cp=0.76

L/B=9.77

B/T=2.21

Considering: L_{wl} in the low range, B_{wl} in high range and T_m in low range

This method decompose the total resistance into components:

$$R_T=(1+k_1)R_F+R_W+R_B+R_{TR}+R_{APP}+R_A$$

Where:

R_T is the total resistance

R_F is the frictional resistance from the ITTC 1957 line

$1+k_1$ is the form factor of bare hull

R_w is the wave resistance of bare hull

R_B is the wave resistance of the bulbous bow

R_{TR} is the additional resistance from the immersed transom

R_{APP} is the resistance due appendage

R_A is the correlation allowance

For the form factor of the hull prediction formula:

$$1+k_1=c_{13} [0.93+c_{12}(B/L_R)^{0.92497}(0.95-C_P)^{-0.521448}(1-C_P+0.0225 \text{ lcb})^{0.6906}],$$

can be used. In this formula C_P is the prismatic coefficient based on the waterline length L and lcb is the longitudinal position of the centre of buoyancy forward of 0.5L as a percentage of L. in the form-facto formula L_R is a parameter reflecting the length of the run according to:

$$L_R/L=1-C_P+0.06C_P\text{lcb}/(4C_P-1)$$

The coefficient C_{12} is defined as:

$C_{12}=(T/L)^{0.2228446}$ when $T/L>0.05$

$C_{12}=48.20(T/L-0.02)^{2.078}+0.479948$ when $0.02<T/L<0.05$

$C_{12}=0.479948$ when $T/L<0.02$

And T is the average moulded draught.

The coefficient C_{13} accounts for the specific shape of the afterbody and is related to the coefficient C_{stern} according to:

$C_{13}=1+0.003C_{stern}$

It depends of the afterbody form, if have a V-shaped section $C_{stern}=-10$, for normal section shape $C_{stern}=0$ and for U-shaped sections with Hogner stern $C_{stern}=+10$.

The wave resistance is determined from:

$$\mathbf{R_W}=c_1c_2c_5\, \nabla\rho\, \exp[m_1F_n{}^d+m_2\cos(\lambda F_n{}^{-2})]$$

With:

$c_1=2223105\, c_7{}^{3.78613}\, (T/B)^{1.07961}(90-i_E)^{-1.37565}$

$c_7=0.229577(B/L)^{0.33333}$ when $B/L<0.11$

$c_7=B/L$ when $0.11<B/L<0.25$

$c_7=0.5-0.0625L/B$ when $B/L>0.25$

$c_2=\exp(-1.89(c_3)^{0.5})$

$c_5=1-0.8A_T/(BTC_M)$